Cell Reports

Article

Triple RNA-Seq Reveals Synergy in a Human Virus-Fungus Co-infection Model

Graphical Abstract

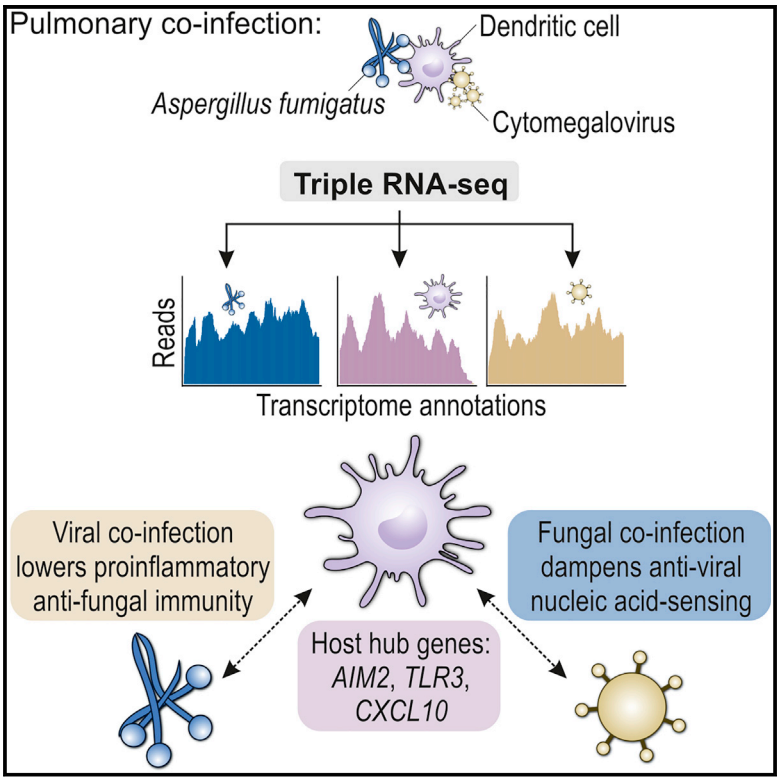

Authors

Bastian Seelbinder, Julia Wallstabe, Lothar Marischen, ..., Alexander J. Westermann, Sascha Schäuble, Juergen Loeffler

Correspondence

loeffler_j@ukw.de

In Brief

Seelbinder et al. demonstrate simultaneous sequencing of RNA isolated from human immune cells infected with *Aspergillus fumigatus* and cytomegalovirus, two pulmonary pathogens regularly affecting the lungs of immunosuppressed patients. They detect characteristic gene expression patterns for single and co-infections and reveal synergistic virulence strategies between the two pathogens.

Highlights

- Triple RNA-seq measures gene expression of co-infected immune cells
- Gene correlation networks reveal different hub gene sets under co-infection
- Co-infection expression includes synergies and interferences between host and pathogens
- Molecular basis of viral/fungal pulmonary infection has potential for the clinic

Seelbinder et al., 2020, Cell Reports *33*, 108389
November 17, 2020
https://doi.org/10.1016/j.celrep.2020.108389

CellPress

Cell Reports

CellPress
OPEN ACCESS

Article

Triple RNA-Seq Reveals Synergy in a Human Virus-Fungus Co-infection Model

Bastian Seelbinder,[1,11] Julia Wallstabe,[2,11] Lothar Marischen,[2,11] Esther Weiss,[2] Sebastian Wurster,[2,3] Lukas Page,[2] Claudia Löffler,[2] Lydia Bussemer,[2] Anna-Lena Schmitt,[2] Thomas Wolf,[1] Jörg Linde,[4] Luka Cicin-Sain,[5,6] Jennifer Becker,[7] Ulrich Kalinke,[7] Jörg Vogel,[8,9] Gianni Panagiotou,[1,10] Hermann Einsele,[2] Alexander J. Westermann,[8,9,11] Sascha Schäuble,[1,11] and Juergen Loeffler[2,11,12,*]

[1]Systems Biology and Bioinformatics, Leibniz Institute for Natural Product Research and Infection Biology – Hans Knöll Institute (HKI), 07745 Jena, Germany

[2]University Hospital Würzburg, Medical Hospital II, WÜ4i, 97080 Würzburg, Germany

[3]The University of Texas MD Anderson Cancer Center, Department of Infectious Diseases, Infection Control and Employee Health, Houston, TX 77030, USA

[4]Friedrich-Loeffler-Institut, Federal Research Institute for Animal Health, Institute of Bacterial Infections and Zoonoses, 07743 Jena, Germany

[5]Department of Vaccinology and Applied Microbiology, Helmholtz Centre for Infection Research, Hannover-Braunschweig Site, 38124 Braunschweig, Germany

[6]Cluster of Excellence RESIST (EXC 2155), Hannover Medical School (MHH) Braunschweig, 38124 Braunschweig, Germany

[7]Institute for Experimental Infection Research, TWINCORE–Centre for Experimental and Clinical Infection Research, a joint venture between the Hannover Medical School and the Helmholtz Centre for Infection Research, Cluster of Excellence RESIST (EXC 2155), Hannover Medical School (MHH), 30625 Hannover, Germany

[8]Institute of Molecular Infection Biology (IMIB), University of Würzburg, 97080 Würzburg, Germany

[9]Helmholtz Institute for RNA-based Infection Research (HIRI), Helmholtz Centre for Infection Research (HZI), 97080 Würzburg, Germany

[10]Department of Medicine and State Key Laboratory of Pharmaceutical Biotechnology, University of Hong Kong, Hong Kong S.A.R., China

[11]These authors contributed equally

[12]Lead Contact

*Correspondence: loeffler_j@ukw.de

https://doi.org/10.1016/j.celrep.2020.108389

SUMMARY

High-throughput RNA sequencing (RNA-seq) is routinely applied to study diverse biological processes; however, when performed separately on interacting organisms, systemic noise intrinsic to RNA extraction, library preparation, and sequencing hampers the identification of cross-species interaction nodes. Here, we develop triple RNA-seq to simultaneously detect transcriptomes of monocyte-derived dendritic cells (moDCs) infected with the frequently co-occurring pulmonary pathogens *Aspergillus fumigatus* and human cytomegalovirus (CMV). Comparing expression patterns after co-infection with those after single infections, our data reveal synergistic effects and mutual interferences between host responses to the two pathogens. For example, CMV attenuates the fungus-mediated activation of pro-inflammatory cytokines through NF-κB (nuclear factor κB) and NFAT (nuclear factor of activated T cells) cascades, while *A. fumigatus* impairs viral clearance by counteracting viral nucleic acid-induced activation of type I interferon signaling. Together, the analytical power of triple RNA-seq proposes molecular hubs in the differential moDC response to fungal/viral single infection or co-infection that contribute to our understanding of the etiology and, potentially, clearance of post-transplant infections.

INTRODUCTION

Allogenic stem cell transplantation (alloSCT) has advanced the therapy of hematological malignancies and is potentially curative for a spectrum of nonmalignant hematological disorders (Singh and McGuirk, 2016). The first successful solid organ transplantation (SOT) took place in 1954; today, transplant statistics are steadily increasing, with over 36,500 organ transplants in the United States in 2018 (based on OPTN data as of January 9, 2019; Harrison et al., 1956). Reduced-intensity conditioning regimes, novel therapeutic strategies to combat graft-versus-host disease, and tailored supportive care have improved alloSCT and SOT outcomes. However, opportunistic infections are still a clinical challenge and a major source of post-transplant complications (Ullmann et al., 2016).

Invasive aspergillosis (IA), predominantly causing pulmonary infections, is responsible for significant post-transplant morbidity, mortality, and incremental cost burdens (Drgona et al., 2014). In addition, human cytomegalovirus (CMV)-associated infections, including CMV pneumonia, remain the most common infectious complications in alloSCT recipients (Camargo and Komanduri, 2017), and CMV viremia is associated

with increased early overall mortality after alloSCT (Green et al., 2016). CMV-disease-related mortality has significantly declined with improved prophylactic medication, PCR-based diagnostics, and pre-emptive antiviral treatment, yet indirect CMV effects continue to adversely impact alloSCT outcomes (de la Cámara, 2016; Duarte and Lyon, 2018). Notably, CMV infections pose an independent risk factor for development of IA in alloSCT recipients (Garcia-Vidal et al., 2008; Marr et al., 2002), and invasive mycoses are a frequent cause of mortality in patients surviving CMV disease (de la Cámara, 2016; Nichols et al., 2002).

Ample evidence indicates that CMV alters the human immune response to escape host surveillance and establish latent persistence (Cheung et al., 2009; Hahn et al., 1998; Kaminski and Fishman, 2016; Kotenko et al., 2000; Taylor-Wiedeman et al., 1991). Several proteins encoded by CMV broadly modulate the magnitude and quality of host immune cell functions (Miller-Kittrell and Sparer, 2009). For example, CMV-secreted immunosuppressive cytokine homologs inhibit dendritic cell maturation and survival as well as dendritic cell-mediated T-helper (Th) cell activation and Th1 differentiation (Chang et al., 2004; Raftery et al., 2004), which are crucial mechanisms for linking innate and adaptive immunity to fungal pathogens. Vice versa, *Aspergillus fumigatus*, the most frequent cause of IA, suppresses human T cell activation in response to CMV (Stanzani et al., 2005). However, the molecular events underlying the differential impact of CMV and *A. fumigatus* on human mononuclear cell functions and the reciprocal immune defense in co-infections are largely unexplored (Grow et al., 2002; Martino et al., 2009; Mikulska et al., 2009; Solak et al., 2013; Upton et al., 2007).

High-throughput RNA sequencing (RNA-seq) has greatly advanced our understanding of infections (Saliba et al., 2017; Colgan et al., 2017) and even allows simultaneous studies of host and pathogen transcriptomes (Westermann et al., 2012). These ''dual RNA-seq'' approaches concurrently isolate host and pathogen RNA, convert it into cDNA libraries for sequencing, and separate the transcriptomes at the computational level by mapping sequencing reads to the respective reference genomes. To date, dual RNA-seq has been applied to diverse infection models to study virulence mechanisms of—and mammalian immune responses to—viral (Juranic Lisnic et al., 2013; Wesolowska-Andersen et al., 2017), bacterial (Westermann et al., 2017), and fungal (Wolf et al., 2018) pathogens as well as eukaryotic parasites (Choi et al., 2014; Pittman et al., 2014). However, multi-organism RNA-seq has not previously been applied to co-infection settings.

Here, we advanced the concept of multi-organism RNA-seq by developing triple RNA-seq, which we applied to human monocyte-derived dendritic cells (moDCs) challenged with the two pulmonary pathogens CMV strain TB40 and *A. fumigatus*. The identified modulations of the host's immunological state upon single infection and co-infection were independently validated by flow cytometry and multiplex cytokine secretion assays. Our collective findings suggest unique interdependencies of CMV and *A. fumigatus* during co-infection that add to our molecular understanding of the synergy between CMV infection and the development of invasive mold infections in immunocompromised patients.

RESULTS

Triple RNA-Seq of Viral/Fungal Co-infections to Simultaneously Study Host and Pathogen Gene Expression

Infection assays of human immune cells with either CMV or *A. fumigatus* were previously established (Paijo et al., 2016; Lother et al., 2014). Here, we built upon these protocols and challenged moDCs with *A. fumigatus* germ tubes or CMV, either separately (single infection) or in combination (co-infection). Host cell viability (Figure S1A), infection rates (Figures S1B and S1C), and morphology (Figure S1D), analyzed by flow cytometry and fluorescence microscopy, demonstrated sustained infections with the pathogens in both single- and co-infection settings. No prominent changes in fungal morphology or infection rate were observed between the two infection settings (Figures S1C and S1D). In contrast, we observed an increased virus infection rate in the presence of *A. fumigatus* as compared to CMV single infection (Figure S1B).

As a prerequisite for multi-organism RNA-seq analysis, several parameters—including lysis conditions, multiplicities of infections (MOIs), and efficient removal of ribosomal RNA (rRNA)—need to be empirically determined for a given infection system. Here, we first established these parameters for single-infection settings of moDCs with either CMV or *A. fumigatus* (Figures S2A–S2C; Data S1). Application of dual RNA-seq to the resulting RNA samples led to the detection of the presumed infection-specific host expression patterns (Figures S2D and S2E), including an induction of pro-inflammatory host marker genes *IL1A/B*, *CCL3*, and *TLR2* upon *A. fumigatus* infection (Braedel et al., 2004; Lass-Flörl et al., 2013; Walsh et al., 2005) and *IFNB* and *CCL2* activation after CMV infection (Loewendorf and Benedict, 2010; McNab et al., 2015). In addition, altered fungal expression levels in the presence of moDCs (Figure S2D), e.g., of the gliotoxin mRNA (*gliF*) that encodes a mycotoxin known to be produced during host infection, as well as induced expression of immunomodulatory viral mRNAs (Figure S2E), further supported the reliability of our approach.

To characterize all three transcriptomes in sequential or simultaneous co-infection settings, we expanded the method toward triple RNA-seq (Figure 1A). MoDCs were either first infected with CMV and, after 4.5 h, additionally with *A. fumigatus*, or first infected with *A. fumigatus* followed by CMV challenge 2 h later, or simultaneously infected with both pathogens. Since dual RNA-seq data indicated that major gene expression changes occurred during the first hours after fungal and viral exposure, co-infection samples were harvested after 9 h and subjected to triple RNA-seq. Co-infection data were compared with transcriptome data from single infections (harvested in parallel with co-infections) and with data from uninfected moDCs or *A. fumigatus* mono-cultures.

We extrapolated sequencing depth requirements for triple RNA-seq to sufficiently cover all three transcriptomes. Since dual RNA-seq indicated host transcriptome coverage to be rate limiting (Figures S2A and S2B), we increased the sequencing depth for triple RNA-seq by ~5-fold, yielding ~15 million non-ribosomal human reads, a threshold above which further increases in sequencing depth have diminishing returns

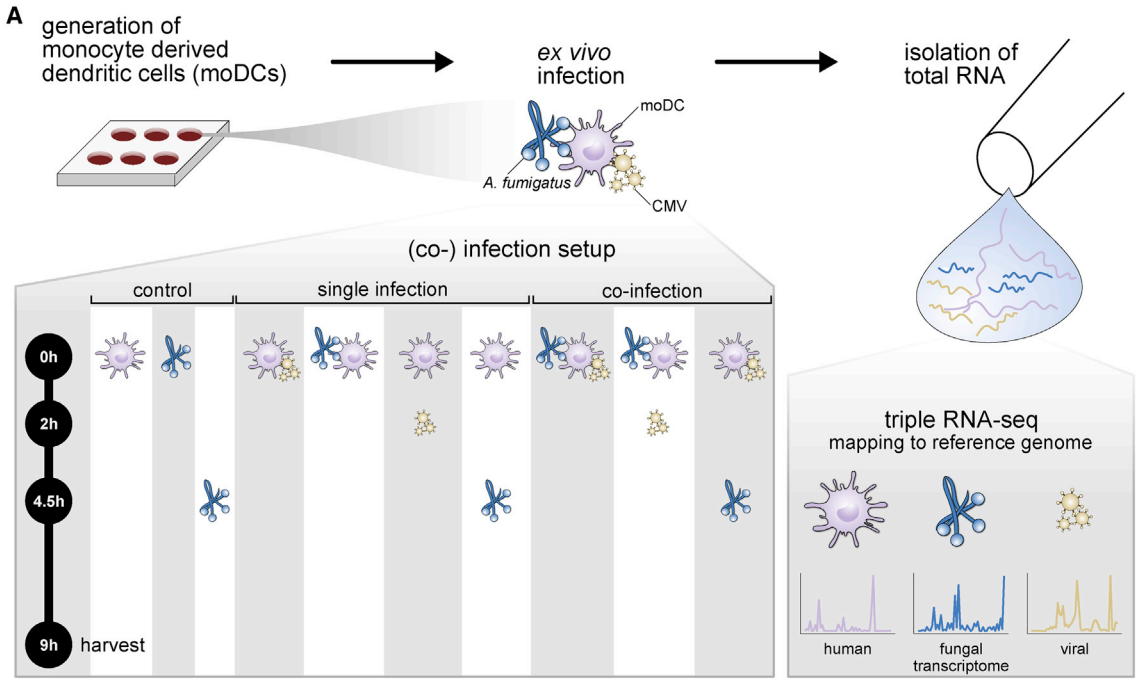

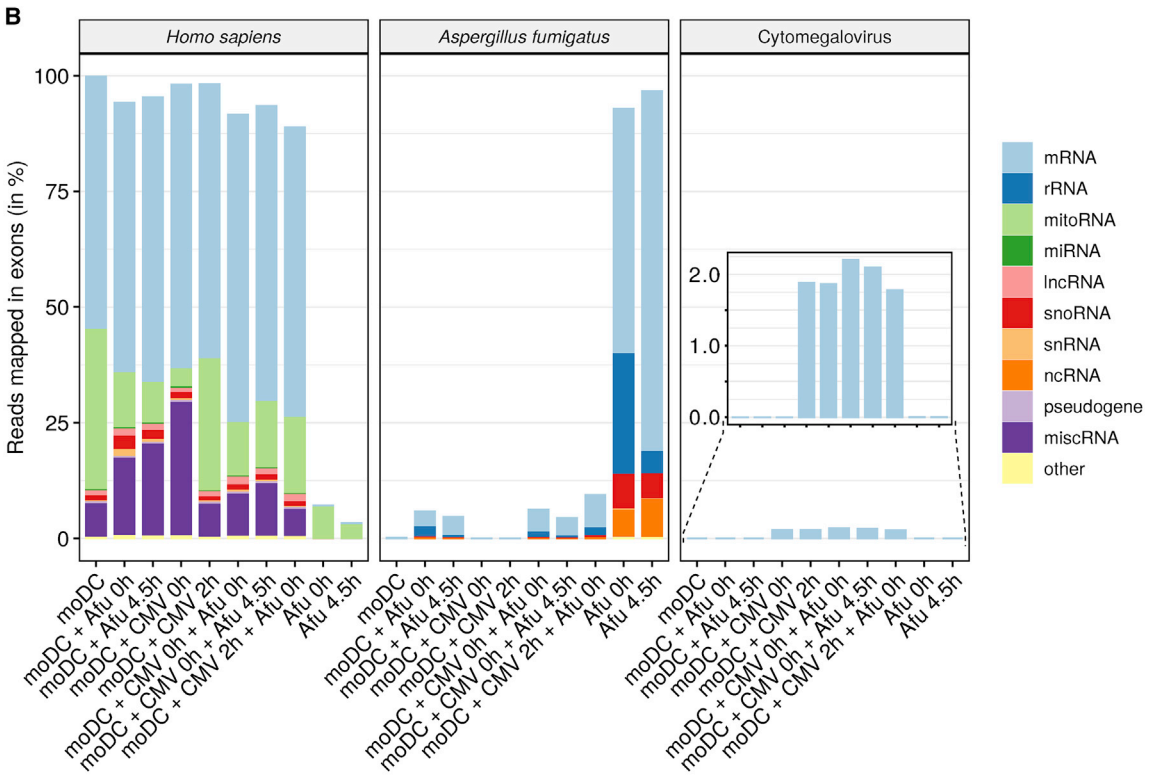

Figure 1. Triple RNA-Seq Outline

(A) Triple RNA-seq pipeline. Setup and time frame for controls, single infection, and co-infection are indicated; n = 4.

(B) Percentages of sequencing reads that mapped to the annotated reference genome of the three studied organisms. Reads per organism were further assigned to the indicated transcript classes. Afu, *Aspergillus fumigatus*; moDC, monocyte-derived dendritic cell; CMV, cytomegalovirus; mitoRNA, mitochondrial RNA; miRNA, microRNA; lncRNA, long noncoding RNA; snoRNA, small nucleolar RNA; snRNA, small nuclear RNA; ncRNA, noncoding RNA; miscRNA, miscellaneous RNA.

(Ching et al., 2014; Liu et al., 2014). Between 67% and 95% of the quality-filtered reads (Data S1; Data S2) were successfully aligned to the reference genomes. While the vast amount of reads mapped to the human genome, *A. fumigatus* contributed up to 24% and CMV contributed up to 1.6% of mapped reads in single-infection and co-infection samples (Figure 1B). As expected, the majority of human (55%) and fungal (55%–75%) reads derived from mRNA. Albeit that ribosomal depletion was less efficient for the fungal than for the human transcriptome, rRNA-derived reads did not exceed 25% in the *A. fumigatus* data subset, allowing for differential gene expression analyses. Other noncoding RNA classes were adequately represented in the two eukaryotic transcriptomes, whereas CMV-annotated genes all encode mRNAs (Figure 1B).

Collectively, these data confirmed the high technical quality of the triple RNA-seq data, with relative proportions of host-to-pathogen read ratios and assignment to major RNA classes matching the predictions extrapolated from the dual RNA-seq pilot (Data S1).

Transcriptomes during Co-infection Differ Globally from Single Infections

Although principal-component analysis (PCA) of moDC transcriptomes revealed no time-point-specific segregation (Figure 2A), distinct clusters were obtained for single-infection conditions with *A. fumigatus* or CMV and co-infection. Similarly, *A. fumigatus* samples failed to cluster according to infection time point yet globally differed between fungal mono-culture and (co-) infection samples (Figure 2B). Finally, CMV transcriptome profiles formed clusters for single infection and co-infection despite the compact size of the CMV genome (166 genes; Figure 2C). In the following, due to the absence of time-point-specific segregation, we disregard temporal information and analyzed infection samples based on etiology (i.e., uninfected, single viral or single fungal infection, and co-infection).

The triple RNA-seq approach potentially reduces systemic noise that may impede cross-species gene expression correlations when separately sampling host and pathogen transcriptomes (Westermann et al., 2017). To globally investigate inter-species co-expression, we calculated node betweenness and degree, two metrics to quantify co-expression network complexity and identify hub genes (Figure 3; Data S3). Focusing on innate immunity-associated effects, we restricted the network analysis to human genes contained within InnateDB (Breuer et al., 2013). The first two networks depicted in Figure 3 show host-pathogen gene-gene correlations present in the intersection of the respective single- and co-infection networks, whereas the remaining networks refer to correlations in the set differences between infection settings. Co-infection networks shared only few cross-species correlations with single-infection networks, whereas co-infection exclusive correlations exhibited a high degree of connectivity and were mostly based on positive correlations. Very few correlations were specific to single *A. fumigatus* infection, but fungus-host connectivity increased during co-infection, suggesting the fungus to adapt to—and maybe benefit from—the presence of CMV. In contrast, the single CMV infection network consisted of many unique, mostly positive, inter-species correlations. This implies a specialized CMV response to human target cells largely ignoring the presence of the fungus.

Cross-species expression correlation analysis can pinpoint host factors with potential as future biomarkers or drug targets. *CXCL11*, for example, showed considerable network importance specifically during co-infection without any obvious correlations in single-infection settings (Data S3). Similarly, *TNF* showed high node degree and betweenness, specifically during co-infection, but occupied a hub position also in the intersection correlation network of fungal single- and co-infection (Data S3). This hints toward a generally important role for tumor necrosis factor (TNF) in the response to *A. fumigatus*, regardless of the additional presence of CMV. *RELA*, in contrast, possesses central network importance in the intersection of CMV single- and co-infection (Data S3), suggesting a particular relevance of this factor in the immune response against CMV.

Differential Gene Expression Profiles in the Three Interacting Organisms

Relative to uninfected moDCs, there was an increased number of differentially expressed human genes upon co-infection as compared to either single infection (Figure S3A). Moreover, we identified specific moDC gene sets with distinct expression patterns between, but low variance within, different infection etiologies (Figure 4A). For example, *TNF*, *IL1A*, and *CXCL8* were specifically upregulated upon the sensing of *A. fumigatus* as previously reported (Balloy et al., 2008; Caffrey-Carr et al., 2017; Caffrey et al., 2015; Cortez et al., 2006; Mehrad et al., 1999; Roilides et al., 1998). On the other hand, induction of *IFNB* (encoding a first-line defense type I interferon [IFN] to CMV infection; Marshall and Geballe, 2009), *CXCL10*, and *CXCL11* (associated with immune clearance in CMV viremia; Cheeran et al., 2003; Knoblach et al., 2011; Murayama et al., 2012) was specific to CMV infection.

The majority of *A. fumigatus* genes differentially expressed in the presence of moDCs compared with the fungal mono-culture were shared between single infection and co-infection (Figure S3B). For example, the *cat1* mRNA that encodes a fungal catalase to break down host-derived hydrogen peroxide was equally highly expressed by *A. fumigatus* during single- and co-infection. This suggests that moDCs were the primary driver of fungal transcriptional reprogramming. This notwithstanding, a greater total number of fungal genes were regulated during single infection than during co-infection, thereby defining an *A. fumigatus* gene set whose regulation might be dispensable for infection in the presence of CMV. CMV expression analysis, on the other hand, revealed largely overlapping sets of differentially expressed viral genes during single infection and co-infection (Figure S3B).

The Host Response to Co-infection Suggests Synergy among *A. fumigatus* and CMV

Closer inspection of moDC expression data identified a subset of key immune pathways whose activity differed markedly between infection settings, including Toll-like receptor (TLR) signaling, nucleic acid sensing, and C-type lectin receptor signaling (Figure S4). In co-infected moDCs, expression levels of *AIM2* and *CCL5*, factors involved in cytosolic DNA sensing (Figure S5) and with known roles in the defense against both fungal and viral

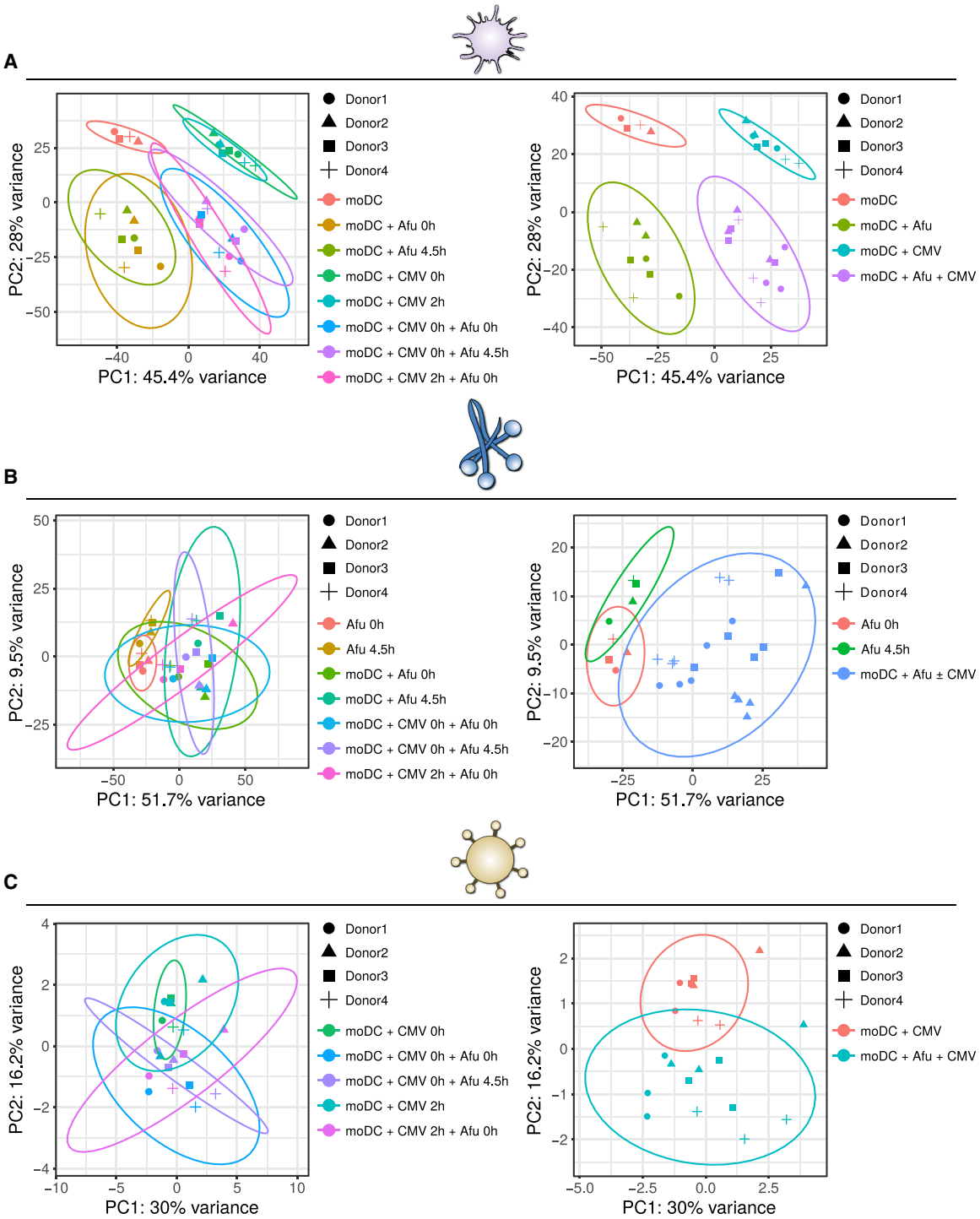

Figure 2. PCA Identifies Co-clustering Transcriptomes

(A–C) PCA for all three organisms after median-by-ratio normalization. Ellipses depict 95% confidence intervals for conditions. PCA for genes associated with (A) *Homo sapiens*, (B) *Aspergillus fumigatus*, or (C) cytomegalovirus (CMV) reference genome. Left: PCAs for all conditions. Right: (A) infection conditions grouped independent of infection time point, (B) data for single infection and co-infection grouped and compared to single-culture *A. fumigatus*, and (C) data for single infection versus co-infection independent of time point. Abbreviations are as explained in the Figure 1 legend.

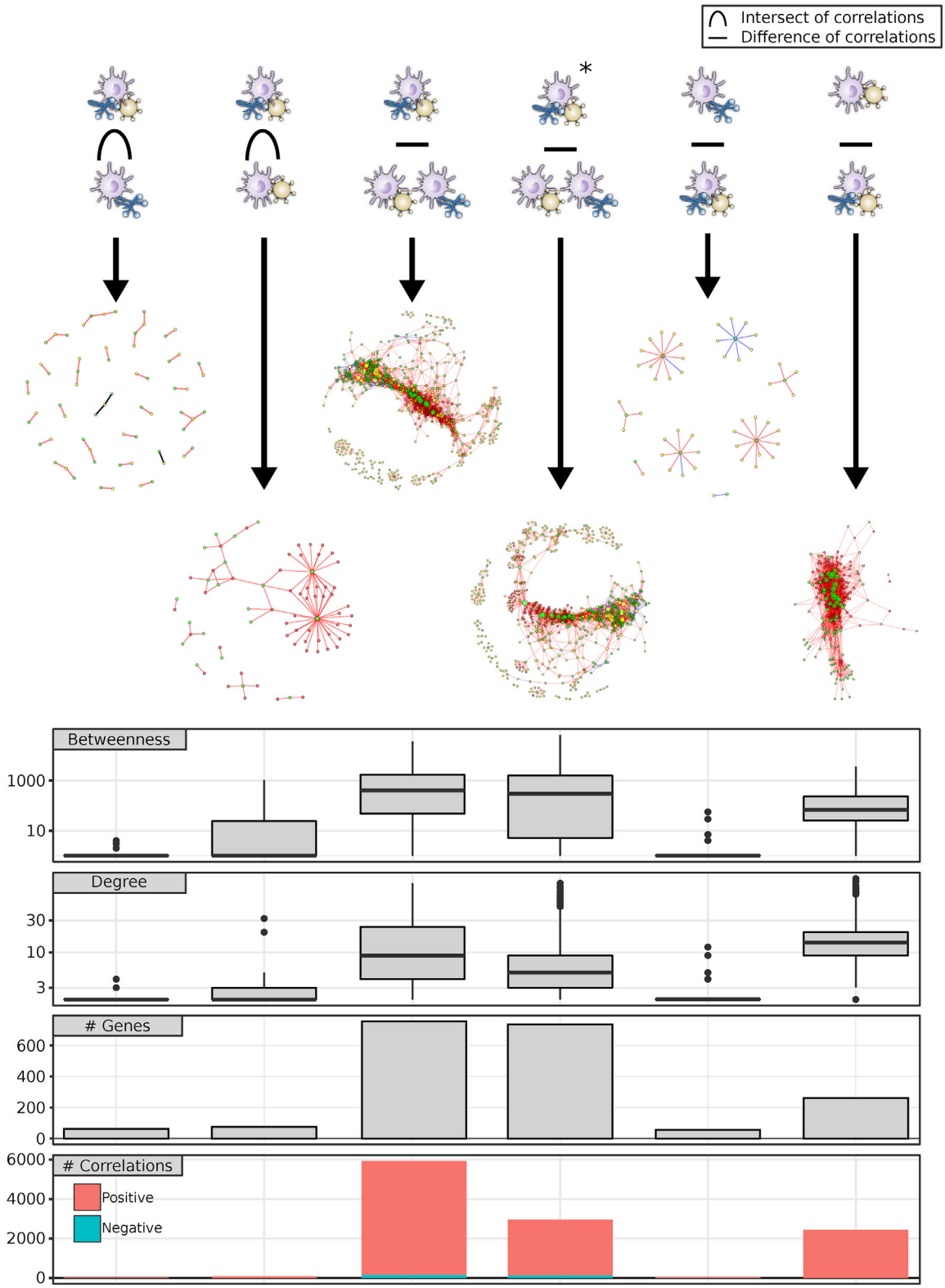

Figure 3. Interspecies Correlation Networks Pinpoint Synergies during Co-infection

Networks indicate significant correlations (edges: $p < 0.05$; $|rho| \geq 0.95$; red indicates positive correlation; and blue indicates negative correlation) of gene expression values (nodes: green represents *Homo sapiens*, yellow indicates *Aspergillus fumigatus*, and red indicates cytomegalovirus [CMV]) between

(legend continued on next page)

infections (Huang and Levitz, 2000; Man et al., 2016; Tyner et al., 2005), matched their cumulative induction after single infections (Figure 4A). However, a number of immune-related moDC genes did not display such additive expression patterns. For instance, the expression of nuclear factor κB (NF-κB)-dependent genes was mainly driven by *A. fumigatus* through TNF signaling (Figure 4B). Co-infection with CMV, however, reduced the expression of those genes as compared to fungal single infection. Similar expression patterns were detected for *IL10* and *IL1B*. Vice versa, RIG-I and ZBP1 signaling (previously associated with type I IFN responses; Onomoto et al., 2010; Yang et al., 2020), as well as expression of *IFNB*, *CXCL10*, and *TLR3*, displayed strong activation upon CMV single infection, which was counteracted by the additional presence of *A. fumigatus* (Figure 4B). The gene for apoptosis-associated speck-like protein (ASC), which is critical for host cell survival upon viral infection (Kumar et al., 2013), was highly expressed in uninfected and CMV-infected moDCs. In contrast, expression of *ASC* was downregulated in the presence of *A. fumigatus*, thereby mirroring the expression pattern of *Dectin-1*, encoding an important fungal infection sensor (Taylor et al., 2007). This points at a disparate role for ASC in response to viral and fungal infections, suggesting an inhibiting effect upon fungal infection that is dominant over the induction upon viral challenge. This hypothesis was further supported by the fact that *IL1B*, despite its functional connection to ASC (Martinon and Tschopp, 2007), was not co-expressed with *ASC*. Finally, *cGAS* and *STING*, both encoding receptors for foreign nucleic acids, and STING also functioning as an IFN-stimulating factor associated with the viral glycoprotein US9 (Choi et al., 2018), were induced upon single CMV infection but downregulated upon co-infection (Figure 4B).

Taken together, these expression data support the existence of two distinct host response patterns to *A. fumigatus* or CMV infection (Figure 4C). Expression of *IL1B, IL10*, and NF-κB-associated genes peaked in *A. fumigatus*-infected moDCs, whereas cGAS, STING, and RIG-I signaling and expression of *IFNB*, *CXCL10*, *TLR3*, and *ZBP1* showed maximal expression upon CMV single infection. Relative to their induction upon the respective single infections, expression levels for all those host genes dropped in co-infected cells, suggesting mutual interfering effects between the two host responses with possibly synergistic effects for the two pathogens.

Independent Validation of Expression Changes

Quantitative real-time PCR measurement of genes from the three organisms that were differentially expressed in the triple RNA-seq data supported the sequencing-derived expression changes (Figure 5A; Figure S5). For instance, differential expression of human *ZBP1*, fungal *cat1*, and the mRNA for the viral envelope glycoprotein UL4 in single infection and co-infection settings could be confirmed in this way (Figure 5A).

We next traced the expression of selected host factors, which were called as differentially expressed in the RNA-seq analysis, on the protein level. For instance, as shown by flow cytometry of antibody-stained moDCs, expression of the surface marker CCR7 was highest after co-infection, which was in line with mRNA levels in the triple RNA-seq dataset (Figure S6). Additionally, altered secretion levels of key cytokines produced from genes that showed pathogen-specific expression patterns were confirmed by multiplex ELISA (Figure 5B; Figure S7). For example, the secreted levels of interleukin (IL)-1β and IFN-β differed between fungal and viral infections (Figure 5B), echoing the differential expression of their cognate mRNAs in the sequencing data.

Altogether, these results underpin the sequencing data, confirm some of the key transcriptomic changes in the infected host cells to extend to the protein level, and provide further support of the notion that pulmonary pathogens differentially affect their host at a global level during co-infection (Reese et al., 2016).

DISCUSSION

Cross-kingdom interactions in polymicrobial infections are increasingly recognized as crucial virulence determinants that shape the outcome of life-threatening infectious diseases (Arvanitis and Mylonakis, 2015; Bergeron et al., 2017). In addition to direct physical interaction and inter-kingdom signaling, altered immunopathology is considered to foster co-infections (Arvanitis and Mylonakis, 2015). Specifically, viral pathogens associated with long-term persistence such as CMV have evolved an armamentarium of counter-strategies to shape-shift the host environment, allowing for immune surveillance evasion and establishment of latent infection (Freeman, 2009; Picarda and Benedict, 2018). Although evidence is limited, previous studies reported broad alterations of host immunity elicited by CMV in immunocompromised patients, entailing the predisposition to subsequent opportunistic fungal diseases (Yong et al., 2018). To improve our understanding of this co-occurrence, we here set out to dissect the molecular interplay of *A. fumigatus*, CMV, and their shared host cells during co-infection.

Establishment of the Triple RNA-Seq Approach

To study the complex interplay of different pathogen classes with their human host and among each other, we implemented the previously proposed concept of multi-organism triple RNA-seq (Westermann et al., 2017). We selected moDCs—being at the border of innate and adaptive immunity—as a host model to establish this technology for a variety of both biological and technical aspects. Myeloid precursors form a reservoir for latent CMV infection and their differentiation into dendritic cells can trigger virus reactivation (Hahn et al., 1998; Jarvis and Nelson, 2002), while moDCs represent a well-studied surrogate model in the context of fungal infection (Hsieh et al., 2017; Mezger et al., 2008; Morton et al., 2011). Additionally, moDCs can be generated in large quantities by well-standardized protocols for the upfront optimization of infection and RNA processing

organisms. The asterisk indicates that correlations between CMV and *A. fumigatus* were removed. Node betweenness and degree are measures of network complexity. Higher degree indicates increased (local) connectivity. Higher betweenness indicates density. Corresponding boxplots show network-wise median (center line), confidence interval (boxes), and quantile (25% and 75%) values. # Genes and # Correlations display numbers of genes and correlation types, respectively.

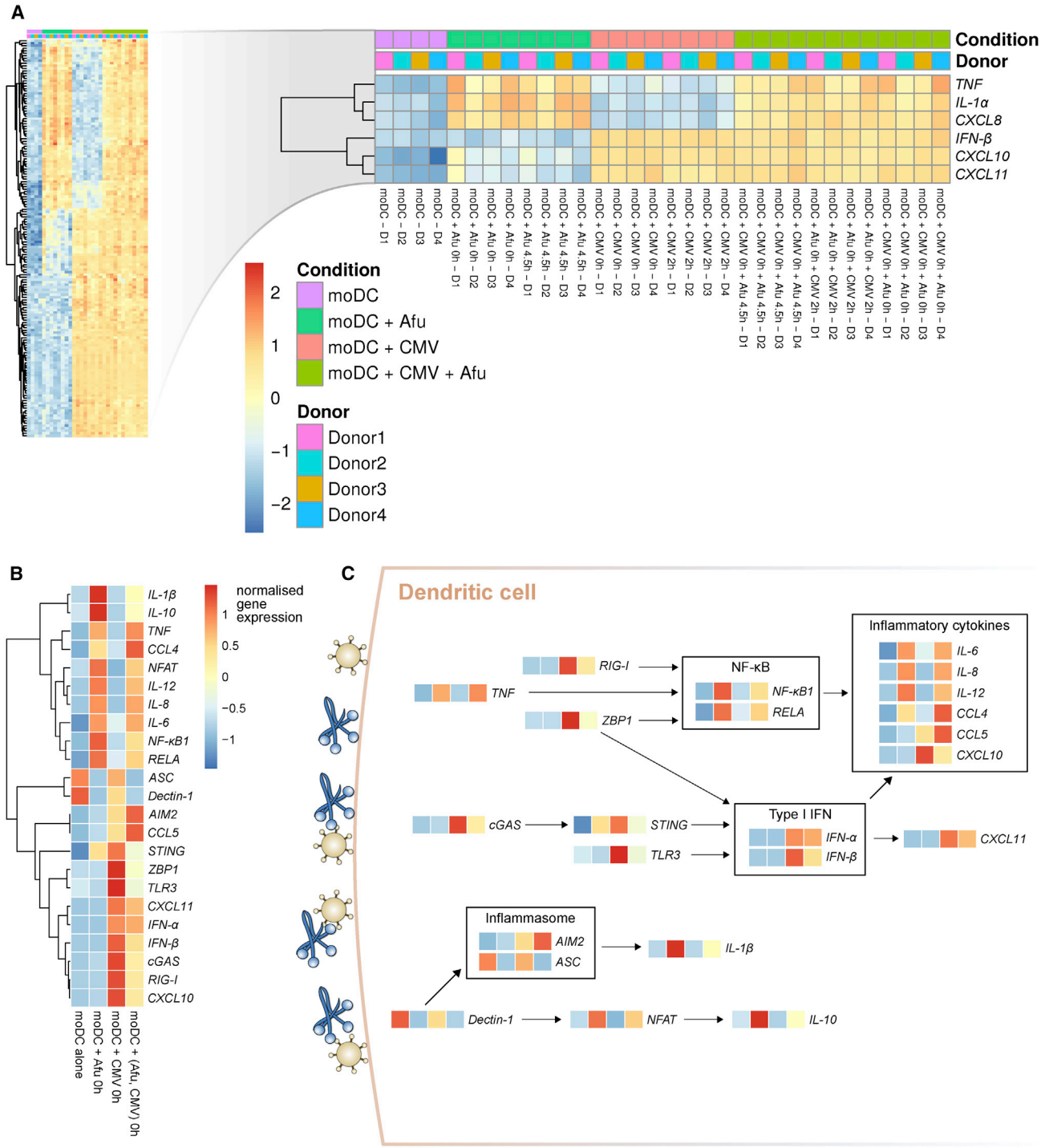

Figure 4. Detailed Differential Gene Expression Analysis of Monocyte-Derived Dendritic Cells

(A) Genes selected for high variance across all conditions and low variance within individual conditions regardless of infection time point. Left: differentially expressed genes (DEGs) with distinct expression patterns across experimental conditions (no stimulation, single infection, and co-infection). Right: examples of innate immune-relevant genes allowing for clear separation of infection types (inferred from innateDB; https://www.innatedb.com/).

(B and C) Selection of host factors involved in monocyte-derived dendritic cell response to cytomegalovirus (CMV), *Aspergillus fumigatus* infection, or co-infection is depicted based on the clustering of similar expression profiles (B) and in topological context (C). Topological analyses are based on Kyoto Encyclopedia of Genes and Genomes reference signaling maps (Figure S4). Abbreviations are as explained in the Figure 1 legend.

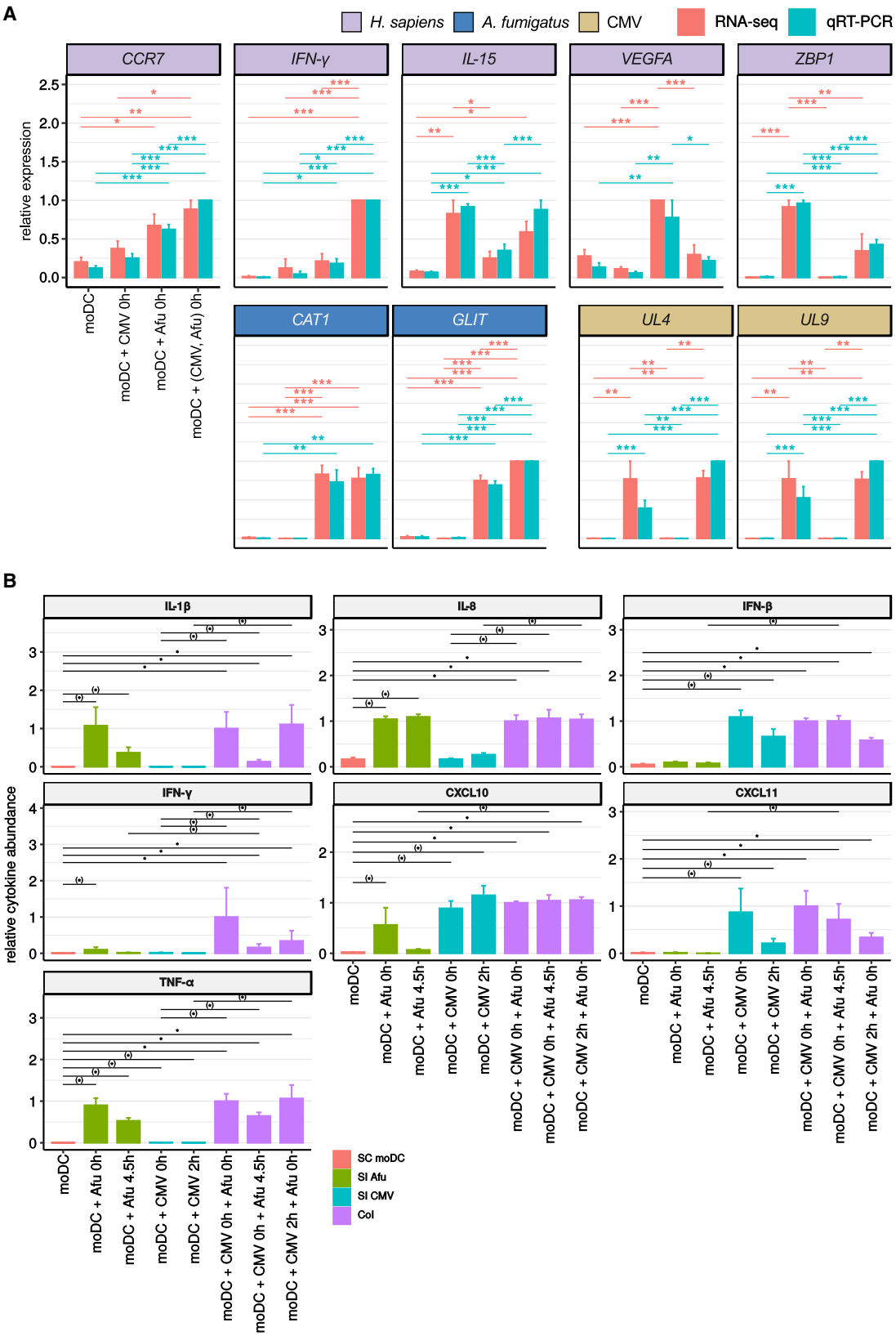

(legend on next page)

protocols and can be analyzed by a variety of phenotypic assays. Despite these advantages, the *ex vivo* transcriptional events described in our study harbor some limitations. These include the fact that a single cell type under well-defined infection conditions in cell culture cannot capture the complex and diverse microenvironments present in, e.g., blood or lung specimens. In consequence, part of the observed transcriptional response might be different in actually co-infected patients, depending again on a large variety of patient-specific factors.

However, the described triple RNA-seq approach potentially provides several advantages over conventional, single-species host or pathogen transcriptomics. Multi-organismal RNA-seq is more resource efficient, reducing costs for cDNA library preparation—the most expensive step in current RNA-seq protocols. Moreover, batch effects may occur during RNA isolation, rRNA depletion, reverse transcription, library generation, or sequencing and can divergently affect host and pathogen transcriptomes when they are treated separately. Batch effects, however, would affect all transcriptomes equally when they are processed in the same reaction. Therefore, subtle interspecies correlations in gene expression that may be masked by technical noise in conventional RNA-seq approaches might be uncovered in multi-organism RNA-seq. This analytical advantage, although not systematically evaluated in this study, was exemplified by the notable number of significant correlations in gene expression across species (Figure 3) and minimal intra-group variance for different infection conditions despite human donor variability (Figure 4A).

Molecular Aspects Underlying the Synergy between Viral and Fungal Pulmonary Infections

Triple RNA-seq recapitulated previously described functional alterations of CMV- and *A. fumigatus*-infected moDCs. Globally, our findings are in line with *in vivo* data showing *A. fumigatus* to drive dendritic cells directly (and indirectly, via polynuclear monocytes) toward a Th17-type immune response (Figure 6A) and showing CMV infection to result in cGAS-STING signaling, leading to an initial production of IFN-α/β, CXCL10, and CXCL11, as well as a subsequent Th1 response (Figures 6A and 6B) (Lio et al., 2016; Paijo et al., 2016; Shankar et al., 2018). Moreover, our results confirmed the CMV-mediated induction of TLR3 signaling and type I IFNs (Mezger et al., 2009) and recapitulated the known upregulation of genes activated through *A. fumigatus*-induced pattern-recognition receptor (PRR) signaling, such as *TNF*, *IL8*, and *IL1B* (Figures 6A and 6C).

Besides, we found several novel mutual interferences within the host response to both pulmonary pathogens under co-infection settings. Specifically, CMV repressed critical PRRs and downstream effectors, including targets essential for mounting a protective anti-*Aspergillus* immune response in high-risk patients (e.g., *CARD9*; Figure 6C). Further, CMV co-infection counteracted *A. fumigatus*-induced upregulation of NF-κB and NFAT (nuclear factor of activated T cells) cascades, resulting in lower induction levels of key proinflammatory cytokines such as IL1B (Figure 6C). This antagonizing effect was particularly pronounced in a scenario when CMV infection preceded *A. fumigatus* exposure (Figure 5B). Thus, whereas most previously described interferences between virus- and fungus-induced host responses were attributed to post-translational alterations caused by CMV proteins (Gredmark-Russ and Söderberg-Nauclér, 2012), our findings showcase the impact of viral co-infection on early transcriptional programs of fungus-exposed dendritic cells.

Conversely, *A. fumigatus* co-infection hampered the induction of viral nucleic-acid-sensing cascades (RIG-I, cGAS, and ZBP1), resulting in reduced expression of *IFNB* and *CXCL10* (Figure 6B), key mediators that are considered predictive for spontaneous CMV clearance in transplant recipients (Lisboa et al., 2015). This may contribute to the increased viral infection rate in *A. fumigatus* co-infected dendritic cells (Figure S1B). Collectively, these observations suggest that *A. fumigatus* and CMV cooperate by mutual interference with host inflammasome activation via downregulation of pathogen-associated molecular patterns by evolutionarily conserved host receptors and signaling cascades. Although not the primary focus of this study, the uncovered transcriptional interferences provide a foundation for guiding future targeted studies in transplant recipients aiming to functionally characterize the clinical implications of these interdependencies.

Exploiting the unique potential of multi-organism RNA-seq, our data simultaneously provide insight into the mutual impact of co-infection on gene expression of the two pathogens. We observed CMV-moDC co-expression networks that were exclusive to single-infection but absent from co-infection settings, and we report correlations between *A. fumigatus* and moDC gene expression that occurred selectively during co-infection (Figure 3). These analyses highlighted human innate immunity-associated genes such as *CXCL10*, *CXCL11*, *AIM2*, and *TLR3* that occupied hub-like positions in the resulting inter-species correlation networks (Figure 3; Data S3). These central positions are exemplified by elevated connectivity to further genes within the correlation networks, suggesting an important role of these genes in information transduction of the immune response to the introduced pathogens. Next to the pathogen-specific expression signature of these genes, the additional network relevance adds to their particular suitability as biomarker candidates to pinpoint viral or fungal presence, but requires further investigation.

Figure 5. Validation on RNA and Protein Level

(A) Comparison of RNA-seq-based and quantitative real-time PCR-based relative expression levels for selected genes. Quantitative real-time PCR-based abundance values normalized to delta-aminolevulinate synthase mRNA (see also Figure S5 for further quantitative real-time PCR validations). RNA-seq-based and quantitative real-time PCR-based gene expression values relative to maximum value per gene per replicate; n = 4.

(B) Relative cytokine concentrations in culture supernatants derived from multiplex ELISA (see also Figure S7 for further measured cytokines). Cytokine levels are relative to co-infection for 9 h. n = 4.

(A and B) Error bars indicate SEM. Asterisks indicate significance level after multiple test correction (false discovery rate; FDR): $^{(*)}p < 0.1$; $^{*}p < 0.05$; $^{**}p < 0.01$; $^{***}p < 0.001$.

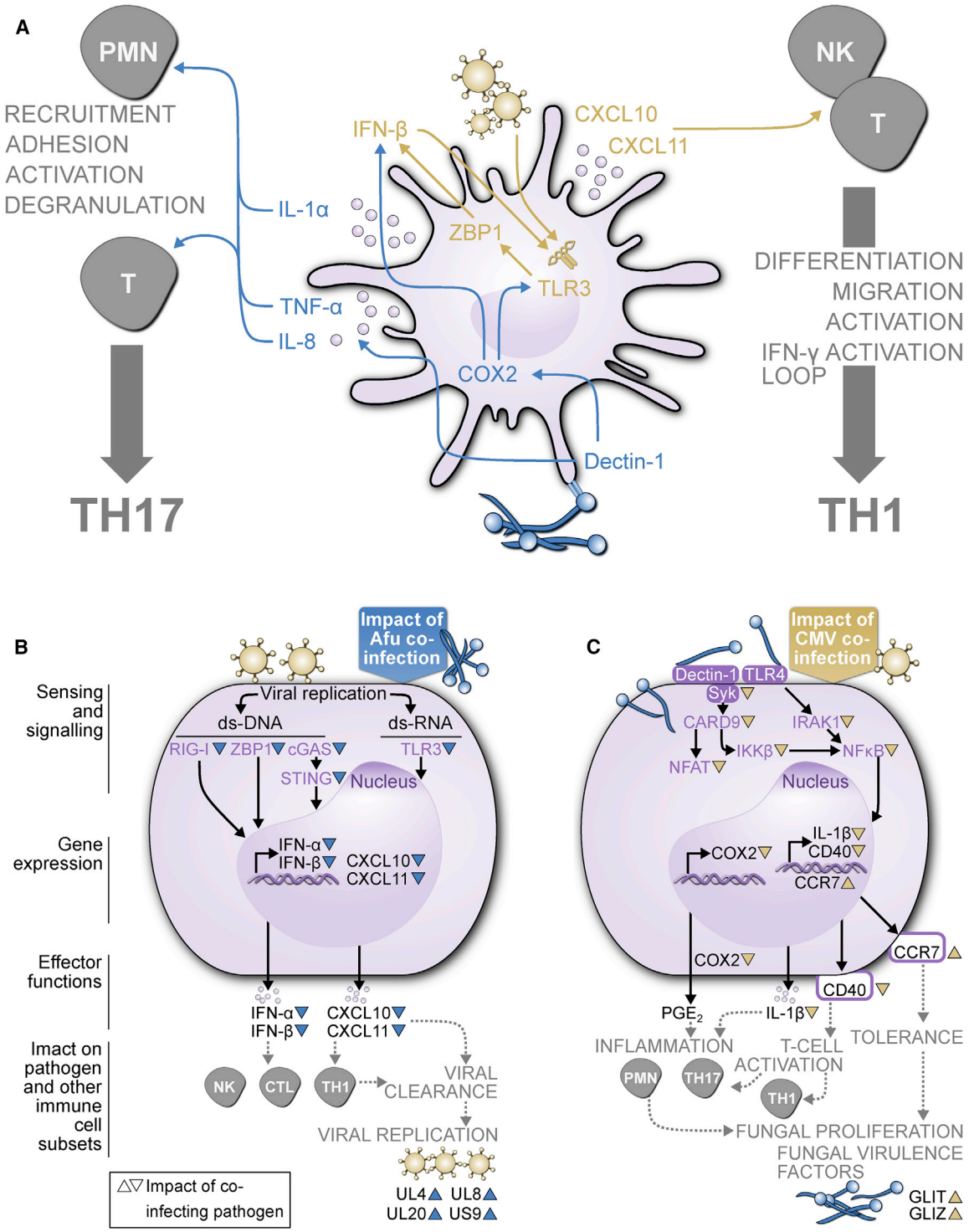

Figure 6. Concerted Defense and Mutual Interference during Co-infection of Monocyte-Derived Dendritic Cells with Fungal and Viral Pathogens

(A) moDC response to fungal and viral challenge. Blue arrows indicate *A. fumigatus*-affected host factors; yellow arrows indicate CMV-affected host factors.

(B) Influence of *A. fumigatus* co-infection on the host response to CMV.

(C) Influence of CMV co-infection on the response to *A. fumigatus*.

PMN, polymorphonuclear leukocytes; NK, natural killer cell; T, lymphocyte T cell; Th, T helper cell; CTL, cytotoxic T cell; CARD9, caspase recruitment domain family member 9; CCR7, C-C motif chemokine receptor 7; cGAS, cyclic GMP-AMP synthase; COX2, cyclooxygenase 2; CXCL, C-X-C motif chemokine ligand;

(legend continued on next page)

The presented triple RNA-seq data represent a rich resource for future exploration. That is, a systematic analysis of expression patterns of human non-immune genes might reveal novel interferences of pulmonary infections with host metabolism, cell cycle, or apoptosis. Moreover, a detailed dissection of differentially expressed fungal or viral genes may lead to the discovery of novel virulence mechanisms in each pathogen.

Perspective

State-of-the-art dual RNA-seq protocols use as few as 10,000 infected cells (Westermann et al., 2017) for ~100–200 ng total RNA, and a similar sensitivity can be expected for the described triple RNA-seq method. This would allow for substantial downscaling of cell samples in the future, allowing for expansion of the analysis to less abundant primary immune cell types such as macrophage and dendritic cell subsets, or alveolar macrophages from bronchoalveolar lavage fluid. Further feasible refinements combining multi-organism RNA-seq and cell sorting or tissue dissection could shift research from the bulk level to phenotypically defined cell populations, for example, to comparatively evaluate transcriptome signatures of infected and uninfected neighboring cells (Westermann and Vogel, 2018). Additionally, triple RNA-seq may be harnessed to investigate the influence of immunosuppressive drugs on co-infected cells or to test how co-infection affects the dendritic cell's ability to cross-present antigens from each pathogen to T cells. Finally, multi-organism RNA-seq holds great promise for expanding our understanding of immune dysregulation in other polymicrobial infections, including post-influenza aspergillosis (Lacoma et al., 2019; Vanderbeke et al., 2018), multifaceted microbial interactions in patients with cystic fibrosis (Sass et al., 2019), or—up-to-the-minute—invasive fungal infections of critically ill coronavirus disease 2019 (COVID-19) patients (Koehler et al., 2020).

In summary, this study established triple RNA-seq to profile transcriptional networks in *A. fumigatus* and CMV infection and to investigate routes of mutual host-pathogen interferences in a co-infection setting. Cost-effectiveness, reproducibility in spite of donor variability, depth, and accuracy propose triple RNA-seq as a powerful tool to probe the emerging concept of direct and immune cell-mediated cross-kingdom inter-dependencies of pathogens in high-risk patients.

STAR★METHODS

Detailed methods are provided in the online version of this paper and include the following:

- KEY RESOURCES TABLE
- RESOURCE AVAILABILITY
  - Lead Contact
  - Materials Availability
  - Data and Code Availability
- EXPERIMENTAL MODEL AND SUBJECT DETAILS
  - Ethics Statement
- METHOD DETAILS
  - Primary cell isolation and differentiation
  - Pulmonary pathogens
  - moDC infection assays
  - Flow cytometry analysis
  - Microscopy
  - Establishment of optimized RNA-seq conditions for single infections
  - RNA extraction, rRNA depletion, cDNA library preparation, and triple RNA-seq
  - Quantitative reverse transcription PCR-based validation of differential gene expression
  - Multiplex cytokine secretion assays
- QUANTIFICATION AND STATISTICAL ANALYSIS
  - RNA-seq data processing
  - Differential gene expression analysis
  - Interspecies and intraspecies gene expression analyses

SUPPLEMENTAL INFORMATION

Supplemental Information can be found online at https://doi.org/10.1016/j.celrep.2020.108389.

ACKNOWLEDGMENTS

The Helmholtz Institute for RNA-based Infection Research (HIRI) supported this work with a seed grant through funds from the Bavarian Ministry of Economic Affairs and Media, Energy and Technology (to J.V., A.J.W., U.K., and J. Loeffler; grant allocation nos. 0703/68674/5/2017 and 0703/89374/3/2017). The study was also financially supported by the Deutsche Forschungsgemeinschaft (DFG) within the Collaborative Research Center CRC124 FungiNet "Pathogenic fungi and their human host: Networks of interaction," DFG project number 210879364 (project A2 to H.E. and J. Loeffler and B5 and INF to G.P.). U.K. received fundings from the DFG Research Unit 2830 (project 04). B.S. and S.S. were supported by the Free State of Thuringia and the European Social Fund (2016 FGR 0053). The authors wish to thank Anne Halenius and Liane Bauersfeld (University Medical Center Freiburg, Institute of Virology, Freiburg, Germany) for providing CMV strain TB40/SE. Furthermore, we would like to thank Bibiane Costa for experimental support and Lea Strobel for technical assistance.

AUTHOR CONTRIBUTIONS

Conceptualization: A.J.W., J. Loeffler, J.V., S.S., and U.K.; Bioinformatics: B.S., J. Linde, S.S., and T.W.; Methodology/Validation: A.-L.S., E.W., J.B., J.W., L.C.-S., L.B., and L.M.; Visualization: A.J.W., B.S., E.W., L.M., S.S., and S.W.; Resources: L.C.-S., J.B., U.K., C.L., and B.S.; Project Administration/Supervision: A.J.W., G.P., H.E., J. Loeffler, S.S., and U.K.; Funding Acquisition: A.J.W., J.V., J. Loeffler, J. Linde, S.S., and U.K.; Writing – Original Draft: A.J.W., B.S., J. Loeffler, J.W., L.M., L.P., S.S., and S.W.; Writing – Review & Editing: all authors.

DECLARATION OF INTERESTS

The authors declare no competing interests.

Dectin-1, C-type lectin domain containing 7A; GLIT/Z, gliotoxin biosynthetic gene cluster; IFN, interferon; IL, interleukin; IKKβ, inhibitor of nuclear factor kappa B kinase subunit beta; IRAK1, interleukin 1 receptor-associated kinase 1; NFAT, nuclear factor of activated T cells; NFκB, nuclear factor κB; PGE_2, prostaglandin E_2; RIG-I, retinoic acid inducible gene I; STING, stimulator of interferon genes; Syk, spleen-associated tyrosine kinase; TLR, Toll-like receptor; TNF-α, tumor necrosis factor alpha; UL, member of RL11 CMV gene family; US9, CMV glycoprotein; ZBP1, Z-DNA-binding protein 1.

Received: February 26, 2020
Revised: July 30, 2020
Accepted: October 23, 2020
Published: November 17, 2020

REFERENCES

Anders, S., and Huber, W. (2010). Differential expression analysis for sequence count data. Genome Biol. *11*, R106.

Arvanitis, M., and Mylonakis, E. (2015). Fungal-bacterial interactions and their relevance in health. Cell. Microbiol. *17*, 1442–1446.

Balloy, V., Sallenave, J.M., Wu, Y., Touqui, L., Latgé, J.P., Si-Tahar, M., and Chignard, M. (2008). Aspergillus fumigatus-induced interleukin-8 synthesis by respiratory epithelial cells is controlled by the phosphatidylinositol 3-kinase, p38 MAPK, and ERK1/2 pathways and not by the toll-like receptor-MyD88 pathway. J. Biol. Chem. *283*, 30513–30521.

Bergeron, A.C., Seman, B.G., Hammond, J.H., Archambault, L.S., Hogan, D.A., and Wheeler, R.T. (2017). Candida albicans and Pseudomonas aeruginosa Interact To Enhance Virulence of Mucosal Infection in Transparent Zebrafish. Infect. Immun. *85*, e00475-17.

Braedel, S., Radsak, M., Einsele, H., Latgé, J.P., Michan, A., Loeffler, J., Haddad, Z., Grigoleit, U., Schild, H., and Hebart, H. (2004). Aspergillus fumigatus antigens activate innate immune cells via toll-like receptors 2 and 4. Br. J. Haematol. *125*, 392–399.

Breuer, K., Foroushani, A.K., Laird, M.R., Chen, C., Sribnaia, A., Lo, R., Winsor, G.L., Hancock, R.E., Brinkman, F.S., and Lynn, D.J. (2013). InnateDB: systems biology of innate immunity and beyond–recent updates and continuing curation. Nucleic Acids Res. *41*, D1228–D1233.

Caffrey, A.K., Lehmann, M.M., Zickovich, J.M., Espinosa, V., Shepardson, K.M., Watschke, C.P., Hilmer, K.M., Thammahong, A., Barker, B.M., Rivera, A., et al. (2015). IL-1α signaling is critical for leukocyte recruitment after pulmonary Aspergillus fumigatus challenge. PLoS Pathog. *11*, e1004625.

Caffrey-Carr, A.K., Kowalski, C.H., Beattie, S.R., Blaseg, N.A., Upshaw, C.R., Thammahong, A., Lust, H.E., Tang, Y.W., Hohl, T.M., Cramer, R.A., and Obar, J.J. (2017). Interleukin 1α Is Critical for Resistance against Highly Virulent Aspergillus fumigatus Isolates. Infect. Immun. *85*, e00661-17.

Camargo, J.F., and Komanduri, K.V. (2017). Emerging concepts in cytomegalovirus infection following hematopoietic stem cell transplantation. Hematol. Oncol. Stem Cell Ther. *10*, 233–238.

Cerqueira, G.C., Arnaud, M.B., Inglis, D.O., Skrzypek, M.S., Binkley, G., Simison, M., Miyasato, S.R., Binkley, J., Orvis, J., Shah, P., et al. (2014). The Aspergillus Genome Database: multispecies curation and incorporation of RNA-Seq data to improve structural gene annotations. Nucleic Acids Res. *42*, D705–D710.

Chang, W.L., Baumgarth, N., Yu, D., and Barry, P.A. (2004). Human cytomegalovirus-encoded interleukin-10 homolog inhibits maturation of dendritic cells and alters their functionality. J. Virol. *78*, 8720–8731.

Cheeran, M.C., Hu, S., Sheng, W.S., Peterson, P.K., and Lokensgard, J.R. (2003). CXCL10 production from cytomegalovirus-stimulated microglia is regulated by both human and viral interleukin-10. J. Virol. *77*, 4502–4515.

Cheung, A.K., Gottlieb, D.J., Plachter, B., Pepperl-Klindworth, S., Avdic, S., Cunningham, A.L., Abendroth, A., and Slobedman, B. (2009). The role of the human cytomegalovirus UL111A gene in down-regulating CD4+ T-cell recognition of latently infected cells: implications for virus elimination during latency. Blood *114*, 4128–4137.

Ching, T., Huang, S., and Garmire, L.X. (2014). Power analysis and sample size estimation for RNA-Seq differential expression. RNA *20*, 1684–1696.

Choi, Y.J., Aliota, M.T., Mayhew, G.F., Erickson, S.M., and Christensen, B.M. (2014). Dual RNA-seq of parasite and host reveals gene expression dynamics during filarial worm-mosquito interactions. PLoS Negl. Trop. Dis. *8*, e2905.

Choi, H.J., Park, A., Kang, S., Lee, E., Lee, T.A., Ra, E.A., Lee, J., Lee, S., and Park, B. (2018). Human cytomegalovirus-encoded US9 targets MAVS and STING signaling to evade type I interferon immune responses. Nat. Commun. *9*, 125.

Colgan, A.M., Cameron, A.D., and Kröger, C. (2017). If it transcribes, we can sequence it: mining the complexities of host-pathogen-environment interactions using RNA-seq. Curr. Opin. Microbiol. *36*, 37–46.

Cortez, K.J., Lyman, C.A., Kottilil, S., Kim, H.S., Roilides, E., Yang, J., Fullmer, B., Lempicki, R., and Walsh, T.J. (2006). Functional genomics of innate host defense molecules in normal human monocytes in response to Aspergillus fumigatus. Infect. Immun. *74*, 2353–2365.

de la Cámara, R. (2016). CMV in Hematopoietic Stem Cell Transplantation. Mediterr. J. Hematol. Infect. Dis. *8*, e2016031.

Drgona, L., Khachatryan, A., Stephens, J., Charbonneau, C., Kantecki, M., Haider, S., and Barnes, R. (2014). Clinical and economic burden of invasive fungal diseases in Europe: focus on pre-emptive and empirical treatment of Aspergillus and Candida species. Eur. J. Clin. Microbiol. Infect. Dis. *33*, 7–21.

Duarte, R.F., and Lyon, S. (2018). Novel approaches to CMV after HCT: report from the 27th European Congress of Clinical Microbiology and Infectious Diseases, Vienna, Austria, 22-25 April 2017. Future Sci. OA *4*, FSO296.

Dunn, W., Chou, C., Li, H., Hai, R., Patterson, D., Stolc, V., Zhu, H., and Liu, F. (2003). Functional profiling of a human cytomegalovirus genome. Proc. Natl. Acad. Sci. USA *100*, 14223–14228.

Freeman, R.B., Jr. (2009). The 'indirect' effects of cytomegalovirus infection. Am. J. Transplant. *9*, 2453–2458.

Garcia-Vidal, C., Upton, A., Kirby, K.A., and Marr, K.A. (2008). Epidemiology of invasive mold infections in allogeneic stem cell transplant recipients: biological risk factors for infection according to time after transplantation. Clin. Infect. Dis. *47*, 1041–1050.

Gredmark-Russ, S., and Söderberg-Nauclér, C. (2012). Dendritic cell biology in human cytomegalovirus infection and the clinical consequences for host immunity and pathology. Virulence *3*, 621–634.

Green, M.L., Leisenring, W., Xie, H., Mast, T.C., Cui, Y., Sandmaier, B.M., Sorror, M.L., Goyal, S., Özkök, S., Yi, J., et al. (2016). Cytomegalovirus viral load and mortality after haemopoietic stem cell transplantation in the era of pre-emptive therapy: a retrospective cohort study. Lancet Haematol. *3*, e119–e127.

Grow, W.B., Moreb, J.S., Roque, D., Manion, K., Leather, H., Reddy, V., Khan, S.A., Finiewicz, K.J., Nguyen, H., Clancy, C.J., et al. (2002). Late onset of invasive aspergillus infection in bone marrow transplant patients at a university hospital. Bone Marrow Transplant. *29*, 15–19.

Hahn, G., Jores, R., and Mocarski, E.S. (1998). Cytomegalovirus remains latent in a common precursor of dendritic and myeloid cells. Proc. Natl. Acad. Sci. USA *95*, 3937–3942.

Harrison, J.H., Merrill, J.P., and Murray, J.E. (1956). Renal homotransplantation in identical twins. Surg. Forum *6*, 432–436.

Hsieh, S.H., Kurzai, O., and Brock, M. (2017). Persistence within dendritic cells marks an antifungal evasion and dissemination strategy of Aspergillus terreus. Sci. Rep *7*, 10590.

Huang, C., and Levitz, S.M. (2000). Stimulation of macrophage inflammatory protein-1alpha, macrophage inflammatory protein-1beta, and RANTES by Candida albicans and Cryptococcus neoformans in peripheral blood mononuclear cells from persons with and without human immunodeficiency virus infection. J. Infect. Dis. *181*, 791–794.

Jarvis, M.A., and Nelson, J.A. (2002). Mechanisms of human cytomegalovirus persistence and latency. Front. Biosci *7*, d1575–d1582.

Juranic Lisnic, V., Babic Cac, M., Lisnic, B., Trsan, T., Mefferd, A., Das Mukhopadhyay, C., Cook, C.H., Jonjic, S., and Trgovcich, J. (2013). Dual analysis of the murine cytomegalovirus and host cell transcriptomes reveal new aspects of the virus-host cell interface. PLoS Pathog. *9*, e1003611.

Kaminski, H., and Fishman, J.A. (2016). The Cell Biology of Cytomegalovirus: Implications for Transplantation. Am. J. Transplant. *16*, 2254–2269.

Kasmapour, B., Kubsch, T., Rand, U., Eiz-Vesper, B., Messerle, M., Vondran, F.W.R., Wiegmann, B., Haverich, A., and Cicin-Sain, L. (2017). Myeloid Dendritic Cells Repress Human Cytomegalovirus Gene Expression and Spread by Releasing Interferon-Unrelated Soluble Antiviral Factors. J. Virol. *92*, e01138-17.

Knoblach, T., Grandel, B., Seiler, J., Nevels, M., and Paulus, C. (2011). Human cytomegalovirus IE1 protein elicits a type II interferon-like host cell response that depends on activated STAT1 but not interferon-γ. PLoS Pathog. *7*, e1002016.

Koehler, P., Cornely, O.A., Böttiger, B.W., Dusse, F., Eichenauer, D.A., Fuchs, F., Hallek, M., Jung, N., Klein, F., Persigehl, T., et al. (2020). COVID-19 associated pulmonary aspergillosis. Mycoses *63*, 528–534.

Kotenko, S.V., Saccani, S., Izotova, L.S., Mirochnitchenko, O.V., and Pestka, S. (2000). Human cytomegalovirus harbors its own unique IL-10 homolog (cmvIL-10). Proc. Natl. Acad. Sci. USA *97*, 1695–1700.

Kumar, M., Roe, K., Orillo, B., Muruve, D.A., Nerurkar, V.R., Gale, M., Jr., and Verma, S. (2013). Inflammasome adaptor protein Apoptosis-associated speck-like protein containing CARD (ASC) is critical for the immune response and survival in west Nile virus encephalitis. J. Virol. *87*, 3655–3667.

Lacoma, A., Mateo, L., Blanco, I., Méndez, M.J., Rodrigo, C., Latorre, I., Villar-Hernandez, R., Domínguez, J., and Prat, C. (2019). Impact of Host Genetics and Biological Response Modifiers on Respiratory Tract Infections. Front. Immunol. *10*, 1013.

Lass-Flörl, C., Roilides, E., Löffler, J., Wilflingseder, D., and Romani, L. (2013). Minireview: host defence in invasive aspergillosis. Mycoses *56*, 403–413.

Latgé, J.P. (1999). Aspergillus fumigatus and aspergillosis. Clin. Microbiol. Rev. *12*, 310–350.

Lio, C.W., McDonald, B., Takahashi, M., Dhanwani, R., Sharma, N., Huang, J., Pham, E., Benedict, C.A., and Sharma, S. (2016). cGAS-STING Signaling Regulates Initial Innate Control of Cytomegalovirus Infection. J. Virol. *90*, 7789–7797.

Lisboa, L.F., Egli, A., Fairbanks, J., O'Shea, D., Manuel, O., Husain, S., Kumar, D., and Humar, A. (2015). CCL8 and the Immune Control of Cytomegalovirus in Organ Transplant Recipients. Am. J. Transplant. *15*, 1882–1892.

Liu, Y., Zhou, J., and White, K.P. (2014). RNA-seq differential expression studies: more sequence or more replication? Bioinformatics *30*, 301–304.

Loewendorf, A., and Benedict, C.A. (2010). Modulation of host innate and adaptive immune defenses by cytomegalovirus: timing is everything. J. Intern. Med. *267*, 483–501.

Lother, J., Breitschopf, T., Krappmann, S., Morton, C.O., Bouzani, M., Kurzai, O., Gunzer, M., Hasenberg, M., Einsele, H., and Loeffler, J. (2014). Human dendritic cell subsets display distinct interactions with the pathogenic mould Aspergillus fumigatus. Int. J. Med. Microbiol. *304*, 1160–1168.

Man, S.M., Karki, R., and Kanneganti, T.D. (2016). AIM2 inflammasome in infection, cancer, and autoimmunity: Role in DNA sensing, inflammation, and innate immunity. Eur. J. Immunol. *46*, 269–280.

Marr, K.A., Carter, R.A., Boeckh, M., Martin, P., and Corey, L. (2002). Invasive aspergillosis in allogeneic stem cell transplant recipients: changes in epidemiology and risk factors. Blood *100*, 4358–4366.

Marshall, E.E., and Geballe, A.P. (2009). Multifaceted evasion of the interferon response by cytomegalovirus. J. Interferon Cytokine Res. *29*, 609–619.

Martino, R., Piñana, J.L., Parody, R., Valcarcel, D., Sureda, A., Brunet, S., Briones, J., Delgado, J., Sánchez, F., Rabella, N., and Sierra, J. (2009). Lower respiratory tract respiratory virus infections increase the risk of invasive aspergillosis after a reduced-intensity allogeneic hematopoietic SCT. Bone Marrow Transplant. *44*, 749–756.

Martinon, F., and Tschopp, J. (2007). Inflammatory caspases and inflammasomes: master switches of inflammation. Cell Death Differ. *14*, 10–22.

McNab, F., Mayer-Barber, K., Sher, A., Wack, A., and O'Garra, A. (2015). Type I interferons in infectious disease. Nat. Rev. Immunol. *15*, 87–103.

Mehrad, B., Strieter, R.M., and Standiford, T.J. (1999). Role of TNF-alpha in pulmonary host defense in murine invasive aspergillosis. J. Immunol. *162*, 1633–1640.

Mezger, M., Kneitz, S., Wozniok, I., Kurzai, O., Einsele, H., and Loeffler, J. (2008). Proinflammatory response of immature human dendritic cells is mediated by dectin-1 after exposure to Aspergillus fumigatus germ tubes. J. Infect. Dis. *197*, 924–931.

Mezger, M., Bonin, M., Kessler, T., Gebhardt, F., Einsele, H., and Loeffler, J. (2009). Toll-like receptor 3 has no critical role during early immune response of human monocyte-derived dendritic cells after infection with the human cytomegalovirus strain TB40E. Viral Immunol. *22*, 343–351.

Mikulska, M., Raiola, A.M., Bruno, B., Furfaro, E., Van Lint, M.T., Bregante, S., Ibatici, A., Del Bono, V., Bacigalupo, A., and Viscoli, C. (2009). Risk factors for invasive aspergillosis and related mortality in recipients of allogeneic SCT from alternative donors: an analysis of 306 patients. Bone Marrow Transplant. *44*, 361–370.

Miller-Kittrell, M., and Sparer, T.E. (2009). Feeling manipulated: cytomegalovirus immune manipulation. Virol. J. *6*, 4.

Morton, C.O., Varga, J.J., Hornbach, A., Mezger, M., Sennefelder, H., Kneitz, S., Kurzai, O., Krappmann, S., Einsele, H., Nierman, W.C., et al. (2011). The temporal dynamics of differential gene expression in Aspergillus fumigatus interacting with human immature dendritic cells in vitro. PLoS ONE *6*, e16016.

Moutaftsi, M., Mehl, A.M., Borysiewicz, L.K., and Tabi, Z. (2002). Human cytomegalovirus inhibits maturation and impairs function of monocyte-derived dendritic cells. Blood *99*, 2913–2921.

Murayama, T., Li, Y., Takahashi, T., Yamada, R., Matsubara, K., Tuchida, Y., Li, Z., and Sadanari, H. (2012). Anti-cytomegalovirus effects of tricin are dependent on CXCL11. Microbes Infect. *14*, 1086–1092.

Nichols, W.G., Corey, L., Gooley, T., Davis, C., and Boeckh, M. (2002). High risk of death due to bacterial and fungal infection among cytomegalovirus (CMV)-seronegative recipients of stem cell transplants from seropositive donors: evidence for indirect effects of primary CMV infection. J. Infect. Dis. *185*, 273–282.

Onomoto, K., Onoguchi, K., Takahasi, K., and Fujita, T. (2010). Type I interferon production induced by RIG-I-like receptors. J. Interferon Cytokine Res. *30*, 875–881.

Paijo, J., Döring, M., Spanier, J., Grabski, E., Nooruzzaman, M., Schmidt, T., Witte, G., Messerle, M., Hornung, V., Kaever, V., and Kalinke, U. (2016). cGAS Senses Human Cytomegalovirus and Induces Type I Interferon Responses in Human Monocyte-Derived Cells. PLoS Pathog. *12*, e1005546.

Picarda, G., and Benedict, C.A. (2018). Cytomegalovirus: Shape-Shifting the Immune System. J. Immunol. *200*, 3881–3889.

Pittman, K.J., Aliota, M.T., and Knoll, L.J. (2014). Dual transcriptional profiling of mice and Toxoplasma gondii during acute and chronic infection. BMC Genomics *15*, 806.

Raftery, M.J., Wieland, D., Gronewald, S., Kraus, A.A., Giese, T., and Schönrich, G. (2004). Shaping phenotype, function, and survival of dendritic cells by cytomegalovirus-encoded IL-10. J. Immunol. *173*, 3383–3391.

Reese, T.A., Bi, K., Kambal, A., Filali-Mouhim, A., Beura, L.K., Bürger, M.C., Pulendran, B., Sekaly, R.P., Jameson, S.C., Masopust, D., et al. (2016). Sequential Infection with Common Pathogens Promotes Human-like Immune Gene Expression and Altered Vaccine Response. Cell Host Microbe *19*, 713–719.

Roilides, E., Dimitriadou-Georgiadou, A., Sein, T., Kadiltsoglou, I., and Walsh, T.J. (1998). Tumor necrosis factor alpha enhances antifungal activities of polymorphonuclear and mononuclear phagocytes against Aspergillus fumigatus. Infect. Immun. *66*, 5999–6003.

Saliba, A.-E., Santos, S.C., and Vogel, J. (2017). New RNA-seq approaches for the study of bacterial pathogens. Curr. Opin. Microbiol. *35*, 78–87.

Sallusto, F., and Lanzavecchia, A. (1994). Efficient presentation of soluble antigen by cultured human dendritic cells is maintained by granulocyte/macrophage colony-stimulating factor plus interleukin 4 and downregulated by tumor necrosis factor alpha. J. Exp. Med. *179*, 1109–1118.

Sampaio, K.L., Weyell, A., Subramanian, N., Wu, Z., and Sinzger, C. (2017). A TB40/E-derived human cytomegalovirus genome with an intact US-gene region and a self-excisable BAC cassette for immunological research. Biotechniques *63*, 205–214.

Sass, G., Nazik, H., Penner, J., Shah, H., Ansari, S.R., Clemons, K.V., Groleau, M.C., Dietl, A.M., Visca, P., Haas, H., et al. (2019). Aspergillus-Pseudomonas

interaction, relevant to competition in airways. Med. Mycol. *57* (*Suppl 2*), S228–S232.

Seelbinder, B., Wolf, T., Priebe, S., McNamara, S., Gerber, S., Guthke, R., and Linde, J. (2019). GEO2RNAseq: An easy-to-use R pipeline for complete preprocessing of RNA-seq data. bioRxiv. https://doi.org/10.1101/771063.

Shankar, J., Cerqueira, G.C., Wortman, J.R., Clemons, K.V., and Stevens, D.A. (2018). RNA-Seq Profile Reveals Th-1 and Th-17-Type of Immune Responses in Mice Infected Systemically with Aspergillus fumigatus. Mycopathologia *183*, 645–658.

Singh, A.K., and McGuirk, J.P. (2016). Allogeneic Stem Cell Transplantation: A Historical and Scientific Overview. Cancer Res. *76*, 6445–6451.

Solak, Y., Biyik, Z., Cizmecioglu, A., Genc, N., Ozbek, O., Gaipov, A., and Yeksan, M. (2013). Cytomegalovirus and Aspergillus spp. coinfection in organ transplantation: a case report and review of the literature. CEN Case Rep. *2*, 59–67.

Stanzani, M., Orciuolo, E., Lewis, R., Kontoyiannis, D.P., Martins, S.L., St John, L.S., and Komanduri, K.V. (2005). Aspergillus fumigatus suppresses the human cellular immune response via gliotoxin-mediated apoptosis of monocytes. Blood *105*, 2258–2265.

Taylor, P.R., Tsoni, S.V., Willment, J.A., Dennehy, K.M., Rosas, M., Findon, H., Haynes, K., Steele, C., Botto, M., Gordon, S., and Brown, G.D. (2007). Dectin-1 is required for beta-glucan recognition and control of fungal infection. Nat. Immunol. *8*, 31–38.

Taylor-Wiedeman, J., Sissons, J.G., Borysiewicz, L.K., and Sinclair, J.H. (1991). Monocytes are a major site of persistence of human cytomegalovirus in peripheral blood mononuclear cells. J. Gen. Virol. *72*, 2059–2064.

Tyner, J.W., Uchida, O., Kajiwara, N., Kim, E.Y., Patel, A.C., O'Sullivan, M.P., Walter, M.J., Schwendener, R.A., Cook, D.N., Danoff, T.M., and Holtzman, M.J. (2005). CCL5-CCR5 interaction provides antiapoptotic signals for macrophage survival during viral infection. Nat. Med. *11*, 1180–1187.

Ullmann, A.J., Schmidt-Hieber, M., Bertz, H., Heinz, W.J., Kiehl, M., Krüger, W., Mousset, S., Neuburger, S., Neumann, S., Penack, O., et al.; Infectious Diseases Working Party of the German Society for Hematology and Medical Oncology (AGIHO/DGHO) and the DAG-KBT (German Working Group for Blood and Marrow Transplantation) (2016). Infectious diseases in allogeneic haematopoietic stem cell transplantation: prevention and prophylaxis strategy guidelines 2016. Ann. Hematol. *95*, 1435–1455.

Upton, A., Kirby, K.A., Carpenter, P., Boeckh, M., and Marr, K.A. (2007). Invasive aspergillosis following hematopoietic cell transplantation: outcomes and prognostic factors associated with mortality. Clin. Infect. Dis. *44*, 531–540.

Vanderbeke, L., Spriet, I., Breynaert, C., Rijnders, B.J.A., Verweij, P.E., and Wauters, J. (2018). Invasive pulmonary aspergillosis complicating severe influenza: epidemiology, diagnosis and treatment. Curr. Opin. Infect. Dis. *31*, 471–480.

Walsh, T.J., Roilides, E., Cortez, K., Kottilil, S., Bailey, J., and Lyman, C.A. (2005). Control, immunoregulation, and expression of innate pulmonary host defenses against Aspergillus fumigatus. Med. Mycol. *43* (*Suppl 1*), S165–S172.

Wesolowska-Andersen, A., Everman, J.L., Davidson, R., Rios, C., Herrin, R., Eng, C., Janssen, W.J., Liu, A.H., Oh, S.S., Kumar, R., et al. (2017). Dual RNA-seq reveals viral infections in asthmatic children without respiratory illness which are associated with changes in the airway transcriptome. Genome Biol. *18*, 12.

Westermann, A.J., and Vogel, J. (2018). Host-Pathogen Transcriptomics by Dual RNA-Seq. Methods Mol. Biol. *1737*, 59–75.

Westermann, A.J., Gorski, S.A., and Vogel, J. (2012). Dual RNA-seq of pathogen and host. Nat. Rev. Microbiol. *10*, 618–630.

Westermann, A.J., Barquist, L., and Vogel, J. (2017). Resolving host-pathogen interactions by dual RNA-seq. PLoS Pathog. *13*, e1006033.

Wiertz, E.J., Jones, T.R., Sun, L., Bogyo, M., Geuze, H.J., and Ploegh, H.L. (1996). The human cytomegalovirus US11 gene product dislocates MHC class I heavy chains from the endoplasmic reticulum to the cytosol. Cell *84*, 769–779.

Wolf, T., Kämmer, P., Brunke, S., and Linde, J. (2018). Two's company: studying interspecies relationships with dual RNA-seq. Curr. Opin. Microbiol. *42*, 7–12.

Yang, D., Liang, Y., Zhao, S., Ding, Y., Zhuang, Q., Shi, Q., Ai, T., Wu, S.Q., and Han, J. (2020). ZBP1 mediates interferon-induced necroptosis. Cell. Mol. Immunol. *17*, 356–368.

Ye, J., Coulouris, G., Zaretskaya, I., Cutcutache, I., Rozen, S., and Madden, T.L. (2012). Primer-BLAST: a tool to design target-specific primers for polymerase chain reaction. BMC Bioinformatics *13*, 134.

Yong, M.K., Slavin, M.A., and Kontoyiannis, D.P. (2018). Invasive fungal disease and cytomegalovirus infection: is there an association? Curr. Opin. Infect. Dis. *31*, 481–489.

STAR★METHODS

KEY RESOURCES TABLE

REAGENT or RESOURCE	SOURCE	IDENTIFIER
Antibodies		
anti-human CD40-PE-Vio®770 (recombinant human IgG1, REAfinity)	Miltenyi Biotec, Bergisch Gladbach, Germany	Cat#130-110-948, Clone: monoclonal REA733; RRID:AB_2658003
anti-human CD80-APC (recombinant human IgG1, REAfinity)	Miltenyi Biotec, Bergisch Gladbach, Germany	Cat#130-117-719, Clone: monoclonal REA661; RRID:AB_2751414
anti-human CD209-VioBlue® (recombinant human IgG1, REAfinity)	Miltenyi Biotec, Bergisch Gladbach, Germany	Cat#130-110-456, Clone: monoclonal REA617; RRID:AB_2656252
anti-human CCR7-VioBlue® (recombinant human IgG1, REAfinity)	Miltenyi Biotec, Bergisch Gladbach, Germany	Cat#130-117-353, Clone: monoclonal REA546; RRID:AB_2733933
anti-human TLR2-PE-Vio®770 (recombinant human IgG1, REAfinity)	Miltenyi Biotec, Bergisch Gladbach, Germany	Cat#130-099-022, Clone: monoclonal REA109; RRID:AB_2656975
anti-human TLR3-APC (mouse IgG1κ)	Miltenyi Biotec, Bergisch Gladbach, Germany	Cat#130-096-885, Clone: monoclonal TLR3.7; RRID:AB_2660004
Bacterial and Virus Strains		
human CMV strain TB40/E-mNeonGreen	Helmholtz Centre for Infection Research, Braunschweig, Germany Kasmapour et al., 2017	https://www.helmholtz-hzi.de
human CMV strain TB40/SE	University Freiburg, Medical Center, Institute of Virology, Freiburg, Germany; Sampaio et al., 2017	https://www.uniklinik-freiburg.de/de.html
Biological Samples		
Human peripheral venous blood from healthy adult donors for generation of monocyte-derived dendritic cells	Paijo et al., 2016; Sallusto and Lanzavecchia, 1994	N/A
Chemicals, Peptides, and Recombinant Proteins		
RNAprotect® Cell Reagent	QIAGEN, Hilden, Germany	Cat#76526
Viobility 405/520 Fixable Dye	Miltenyi Biotec, Bergisch Gladbach, Germany	Cat#130-109-814
iTaq Universal SYBR® Green Supermix	Bio-Rad Laboratories GmbH, Feldkirchen, Germany	Cat#1725124
Recombinant human IL-4, premium grade	Miltenyi Biotec, Bergisch Gladbach, Germany	Cat#130-093-922
Recombinant human GM-CSF,premium grade	Miltenyi Biotec, Bergisch Gladbach, Germany	Cat#130-093-866
Critical Commercial Assays		
RiboPure-Yeast Kit	Thermo Fisher Scientific, Waltham, MA, USA	Cat#AM1926
DNase I, RNase free (1.000 U)	Thermo Fisher Scientific, Waltham, MA, USA	Cat#EN0521
M-MLV reverse transcriptase	Invitrogen, Carlsbad, CA, USA	Cat#28025013
cDNA First Strand Synthesis Kit	Thermo Fisher Scientific, Waltham, MA, USA	Cat#K1612
Ribo-Zero Gold rRNA removal kit (human, mouse, rat) (24 reactions)	Illumina, San Diego, CA, USA	Cat#MRZG12324
ProcartaPlex 16-plex Immunoassay (IFN-α, IFN-β, IFN-γ, IL-1α, IL-1β, IL-2, IL-6, IL-8, IL-10, IL-12p70, IL-17A, IL-23, CXCL10, CXCL11, CCL5, TNF-α)	Thermo Fisher Scientific, Waltham, MA, USA	Cat#PPX-16, customized

(*Continued on next page*)

Continued

REAGENT or RESOURCE	SOURCE	IDENTIFIER
Deposited Data		
Triple RNA-seq, *A. fumigatus*, CMV and *H. sapiens*	https://www.ncbi.nlm.nih.gov/geo/	GSE134344
Dual RNA-seq *A. fumigatus* and *H. sapiens*	https://www.ncbi.nlm.nih.gov/geo/	GSE135450
Dual RNA-seq CMV and *H. sapiens*	https://www.ncbi.nlm.nih.gov/geo/	GSE136217
Experimental Models: Organisms/Strains		
Aspergillus fumigatus (wildtype)	ATCC	ATCC: 46645
Aspergillus fumigatus dTomato	ATCC; Lother et al., 2014	ATCC: 46645
Aspergillus fumigatus GFP	ATCC; Lother et al., 2014	ATCC: 46645
Oligonucleotides		
See Table S1 for primer sequences (ALAS1, IL15, CCR7, ZBP1, VEGFA, IFNG, TLR3, CD40, GliT, GliZ, Ilv3, Cat1, SrbA, UL4, UL8, UL20, US16, UL9, US9)	This paper	N/A
Software and Algorithms		
CellQuest Pro Software (Becton & Dickinson)	https://www.bd.com/en-us	Becton & Dickinson, Franklin Lakes, NJ, USA
FACSDiva Software	https://www.bd.com/en-us	Becton & Dickinson, Franklin Lakes, NJ, USA
FlowJo Software, v10	https://www.flowjo.com; https://www.bd.com/en-us	Treestar/ Becton & Dickinson, Ashland, OR, USA
FCS Express Software, v7	https://denovosoftware.com	De Novo Software, Pasedena, CA, USA
NIS Elements Imaging software, v5.02.00	https://www.microscope.healthcare.nikon.com	Nikon Instruments, Amsterdam, Netherlands
R	https://cran.r-project.org/	3.5.1
featureCounts	https://cran.r-project.org/	Rsubread 1.28.0
DESeq	https://bioconductor.org	1.30.0
DESeq2	https://bioconductor.org	1.18.1
limma voom	https://bioconductor.org	3.34.6
edgeR	https://bioconductor.org	3.20.7
geo2RNaseq	https://singularity-hub.org/accounts/login/?next=/collections/4387; https://bitbucket.org/Xentrics/geo2rnaseq/src/master/	0.9.12
FastQC	https://www.bioinformatics.babraham.ac.uk/projects/fastqc/	0.11.8
Trimmomatic	http://www.usadellab.org/cms/?page=trimmomatic	0.36
HiSat2	https://daehwankimlab.github.io/hisat2/	2.1.0
SAMtools	https://www.htslib.org/	1.7
MultiQC	https://multiqc.info/	1.5
Jupyter	https://jupyter.org/	4.4.0
Tidyverse	https://cran.r-project.org/	1.2.1
Magrittr	https://cran.r-project.org/	1.5.0
Reshape2	https://cran.r-project.org/	1.4.4
ggplot2	https://cran.r-project.org/	3.1.1
Ggpubr	https://cran.r-project.org/	0.2.5
Ggsci	https://cran.r-project.org/	2.9
Dplyr	https://cran.r-project.org/	0.7.6
Tidyr	https://cran.r-project.org/	1.3.1
Stringr	https://cran.r-project.org/	1.3.0

(*Continued on next page*)

Continued

REAGENT or RESOURCE	SOURCE	IDENTIFIER
AnnotationDbi	https://bioconductor.org	1.44.0
org.Hs.eg.db	https://bioconductor.org	3.10.0
setRank	https://cran.r-project.org/	1.1.0
Pathview	https://bioconductor.org	1.26.0
Pheatmap	https://cran.r-project.org/	1.0.12
igraph	https://cran.r-project.org/	1.2.5
WriteXLS	https://cran.r-project.org/	5.0.0
corrplot	https://cran.r-project.org/	0.84
RcolorBrewer	https://cran.r-project.org/	1.1-2
enrichR	https://cran.r-project.org/	2.1.0
cowplot	https://cran.r-project.org/	1.1.0
Other		
H. sapiens reference genome	https://www.ncbi.nlm.nih.gov/	GRCH 38 v89
A. fumigatus Af293 reference genome	http://www.aspergillusgenome.org/	s03-m05-r09
CMV reference genome	https://www.ncbi.nlm.nih.gov/	EF999921.1

RESOURCE AVAILABILITY

Lead Contact

Further information and requests for resources and reagents should be directed to and will be fulfilled by the Lead Contact, Juergen Loeffler (loeffler_j@ukw.de).

Materials Availability

All primary material generated in this study will be made available upon request following publication. A completed Materials Transfer Agreement might be necessary, especially if there is potential for commercial application.

Data and Code Availability

All primary sequencing data and processed data described in this manuscript have been deposited in the NCBI Gene Expression Omnibus under the accession numbers GEO: GSE134344, GSE135450 and GSE136217.

Code for preprocessing RNA sequencing data and analysis is deposited and available at https://github.com/SchSascha/manuscript_tripleRNAseq.

EXPERIMENTAL MODEL AND SUBJECT DETAILS

Healthy blood donors were exclusively in the age between 18-59 years and otherwise excluded from providing blood samples. Both sexes were included in the study equally and at random; the sex of the blood donors was anonymised and represents the normal distribution within this population.

Ethics Statement

The processing of human peripheral venous blood from healthy adult donors was approved by the Ethical Committee of the University Hospital Würzburg (#302/12).

METHOD DETAILS

Primary cell isolation and differentiation

To generate moDCs, monocytes were isolated from leukoreduction system chambers containing blood from healthy volunteers and standard density-gradient centrifugation followed by positive selection using magnetic-activated cell sorting (CD14 MicroBeads, human, Miltenyi Biotec). Monocytes were cultured in CellGenix GMP dendritic cell medium (serum-free, CellGenix) supplemented with 120 μg gentamicin (Refobacin, Merck) in 24-well plates with 1×10^6 cells/ml. Cells were differentiated for 6 days by addition of 1,000 U/ml granulocyte macrophage-colony stimulating factor (Miltenyi Biotec) and 1,000 U/ml interleukin (IL)-4 (Miltenyi Biotec) (Mezger et al., 2008; Paijo et al., 2016; Sallusto and Lanzavecchia, 1994).

Pulmonary pathogens

Reporter strain human CMV TB40/E-mNeonGreen and CMV TB40/SE (non-fluorescent) were generated according to published protocols (Kasmapour et al., 2017; Paijo et al., 2016; Sampaio et al., 2017). *A. fumigatus* (ATCC 46645) germ tubes were prepared overnight in RPMI (Invitrogen) and used for dual or triple RNA-seq. For flow cytometry and microscopy (see below), dTomato- or GFP-expressing *A. fumigatus* germ tubes were used.

moDC infection assays

Primary human cells were infected with CMV at a multiplicity of infection (MOI) 3 and with subsequent centrifugal enhancement at 300 x *g* for 30 min. *A. fumigatus* germ tubes, which represent an invasive immunogenic morphotype of the fungus, were added at MOI 0.5. For co-infections, pathogens were added simultaneously or subsequently (Figure 1A). After harvesting, cells were centrifuged and pellets collected in HBSS (Invitrogen) or RNA*protect* Cell Reagent (QIAGEN), and cell-free supernatants were stored at −80°C. For flow cytometry and microscopy, (see below) moDCs were infected with CMV for 24 h before adding germ tubes, because detection of NeonGreen fluorescence in infected cells requires sufficient replication of the virus.

Flow cytometry analysis

CMV and *A. fumigatus* infection rates were determined by flow cytometry, measuring fluorescent signals of moDCs positive for mNeonGreen (CMV) or GFP (*A. fumigatus*), respectively (Figures S1B and S1C). Viability of moDCs was determined by staining with Viobility 405/520 Fixable Dye (Miltenyi Biotec), defining negative populations as viable. Additionally, cells were stained with anti-CD40-PE-Vio770 (REA733, Miltenyi Biotec), anti-CD80-APC (REA661, Miltenyi Biotec), anti-CD209-VioBlue, (REA617, Miltenyi Biotec), anti-CCR7-VioBlue (REA546, Miltenyi Biotec), anti-TLR2-PE-Vio770 (REA109, Miltenyi Biotec) or anti-TLR3-APC (TLR3.7, Miltenyi Biotec). Mean fluorescence intensities of these surface markers were measured and isotypes subtracted. Data were acquired on a FACSCalibur using CellQuest Software (Becton & Dickinson) or FACSCanto II using FACSDiva software (Becton & Dickinson). Data analysis was done with FlowJo (Treestar/Becton & Dickinson, version 10) or FCS Express 7 (*De Novo* Software).

Microscopy

Morphology and fluorescence signals for CMV (mNeonGreen) or *A. fumigatus* (dTomato) were analyzed in 48-well cell culture plates using a Nikon Eclipse Ti microscope (Nikon) with an Okolab incubator set at 37°C. Images were obtained at 20-fold magnification and processed using NIS Elements Imaging software (Nikon, version 5.02.00).

Establishment of optimized RNA-seq conditions for single infections

As a prerequisite for multi-organism RNA-seq analysis in our infection model, lysis conditions should be sufficiently harsh to disrupt cellular membranes of all interacting organisms, but sufficiently mild to maintain high RNA integrity. Additionally, multiplicities of infection (MOIs) must be adjusted to ensure homogeneous coverage of individual transcriptomes in the resulting sequencing data. That is, the relative proportions of transcriptomes in isolated RNA samples should match the ratio of the respective genome sizes. Therefore, we first evaluated yield and quality of RNA isolated from moDCs infected with either *A. fumigatus* or CMV at different time points and MOIs, and observed high RNA integrity (RIN > 7) for all conditions (Figures S2A and S2B).

While highly abundant in any organism (> 90% of total cellular RNA), ribosomal RNA (rRNA) provides little informative value about cellular physiology. Therefore, ribosomal transcripts are typically depleted from sequencing libraries, either by active rRNA pull-out (e.g., Ribo-Zero technology) or enrichment of polyadenylated transcripts. In principle, both options are suitable for our infection model, since mRNAs of all three interacting organisms are polyadenylated. We found that both approaches efficiently depleted human ribosomal reads (Figure S2C). However, to retain potentially interesting non-polyadenylated transcripts (e.g., microRNAs [miRNAs], small nucle(ol)ar RNAs [snRNAs, snoRNAs] and polyA- long noncoding RNAs [lncRNAs]; Figure S2C), we employed Ribo-Zero technology for further RNA-seq experiments.

After rRNA removal from single-infection samples, cDNA libraries were prepared and sequenced to shallow depth (~5-8 million reads/library) for initial quality assessment. Obtained sequencing reads aligned to their parental reference genome with little cross-mapping observed (Figures S2A and S2B). In fact, the vast majority of cross-mapped reads derived from mitochondrial genes present in both *Aspergillus* and human cells, and all of these reads were removed from further analyses. As expected, the fungal-to-human read ratio in *Aspergillus*-infected samples increased with MOI. In line with the high proportions of fungal reads (~20% of total mapped reads), human exon coverage was the rate-limiting factor (Figure S2A), thus favoring the low-dose infections (MOI 0.5) for further experiments. While the vast majority of reads in CMV-infected moDCs mapped to the human genome, viral read proportion and exon coverage increased time-dependently, indicative of viral replication (Figure S2B).

Even with the low sequencing depth used in this pilot experiment, the induction of marker genes for human dendritic cell activation and pathogenicity-related fungal genes was detected (Figure S2D). For example, upregulation of *IL-1, CCL3,* and *TLR2* indicated activation of well-described pro-inflammatory cascades in moDCs infected with *Aspergillus* (Braedel et al., 2004; Lass-Flörl et al., 2013; Walsh et al., 2005). Fungal cells also showed elevated expression of genes for toxic molecules such as the gliotoxin GliF (Latgé, 1999). Similarly, expression profiles during virus infection reflected expected patterns (Figure S2E) as CMV-infected moDCs upregulated *IFN-γ* and *CCL2* (Loewendorf & Benedict, 2010; McNab et al., 2015), whereas viral gene expression was generally induced over

time (Figure S2E displays viral expression at two later stages relative to an early infection stage) indicating active proliferation (Dunn et al., 2003; Moutaftsi et al., 2002; Wiertz et al., 1996).

RNA extraction, rRNA depletion, cDNA library preparation, and triple RNA-seq

For extraction of human, fungal and viral RNA, RiboPure RNA Purification Kit yeast (Thermo Fisher Scientific) was used according to the manufacturer's instructions. Total RNA was treated with 0.13 U/μl DNase I (Thermo Fisher Scientific) for 30 min at 37°C to remove contaminating genomic DNA. The integrity of DNase-treated RNA was assessed on a bioanalyzer (Agilent). All samples had RNA integrity numbers (RIN) $\geq$ 7.0. Where explicitly indicated (as polyA$^+$), total RNA was directly converted into first-strand cDNA using an oligo(dT)$_{25}$ primer, fragmented (four 30 s ultrasound pulses), and processed as outlined below. Otherwise, ribosomal transcripts were actively removed using Ribo-Zero Gold rRNA removal kits (human, mouse, rat) (Illumina) following manufacturer's instructions for 500 ng DNase-treated RNA as input for rRNA depletion.

The cDNA libraries for Illumina sequencing were generated by Vertis Biotechnologie AG, Freising-Weihenstephan, Germany, with rRNA-free RNA sheared via ultrasound sonication (four 30 s pulses, 4°C) to generate 200- to 400-nucleotide fragments, on average. Fragments < 20 nucleotides were removed using Agencourt RNAClean XP kits (Beckman Coulter Genomics), and Illumina TruSeq adapters were ligated to the 3′ ends of remaining fragments. First-strand cDNA synthesis was performed using M-MLV reverse transcriptase (NEB) with 3′ adapters used as primer target sites. First-strand cDNA was purified, and 5′ Illumina TruSeq sequencing adapters were ligated to 3′ ends of antisense cDNA. Resulting cDNA was PCR-amplified to about 10 to 20 ng/μl using high-fidelity DNA polymerase. TruSeq barcode sequences were included in 5′ and 3′ TruSeq sequencing adapters. The cDNA libraries were purified using Agencourt AMPure XP kits (Beckman Coulter Genomics) and analyzed by capillary electrophoresis (Shimadzu MultiNA microchip).

For sequencing, cDNA libraries were pooled in approximately equimolar amounts. Pools were size-fractionated to 200-600 bp using differential cleanup with Agencourt AMPure kits (Beckman Coulter Genomics). Aliquots of cDNA pools were analyzed by capillary electrophoresis (Shimadzu MultiNA microchip). Sequencing was performed on a NextSeq 500 platform (Illumina) at Vertis Biotechnologie AG, Freising-Weihenstephan, Germany (single-end mode, 75 cycles).

Quantitative reverse transcription PCR-based validation of differential gene expression

RNA of untreated moDCs or moDCs after infection with CMV, *A. fumigatus* or both was reverse transcribed into cDNA using Thermo Fisher cDNA First Strand Synthesis Kits. Primers (Sigma-Aldrich) were designed using Primer-Blast (Ye et al., 2012) and The Aspergillus Genome Database (Cerqueira et al., 2014), avoiding the occurrence of target sequences in the other two organisms (Table S1). Quantitative reverse transcription (qRT)-PCR was conducted using SYBRGreen Master Mix from (BioRad) in a Step One System (Applied Biosystems). Primer specificity was confirmed by agarose (Roth) gel electrophoresis (Serva) of PCR amplicons using ethidium bromide (Thermo Fisher). Gel images were documented in a Multi-Image Light Cabinet (Alpha Innotech).

Multiplex cytokine secretion assays

Cell culture supernatants were analyzed by multiplex cytokine secretion assays according to the manufacturer's instructions using 16-plex ProcartaPlex Immunoassays (Thermo Fisher Scientific) including IFN-α, IFN-β, IFN-γ, IL-1α, IL-1β, IL-2, IL-6, IL-8, IL-10, IL-12p70, IL-17A, IL-23, CXCL10, CXCL11, CCL5, and TNF-α.

Cytokines with concentration levels above measurement range were set to 1.05 times the maximum. Concentration levels below measurement range or negative concentrations were set to 0. Significant changes in the concentration of cytokines were determined using pairwise two-sided Wilcoxon rank-sum tests. P values for each test were adjusted for multiple testing using FDR. We rejected the null hypothesis for FDR < 0.1.

QUANTIFICATION AND STATISTICAL ANALYSIS

RNA-seq data processing

Preprocessing of raw reads including quality control and gene abundance estimation was done with GEO2RNaseq pipeline version 0.9.12 in *R* version 3.5.1 (Seelbinder et al., 2019). Quality analysis was done with FastQC version 0.11.8 before and after trimming. Read-quality trimming was done with Trimmomatic version 0.36. Adaptor sequences were removed, window size trimming performed (15 nucleotides, average Q < 25) including 5′ and 3′ per-base trimming for Q < 3 and removal of sequences shorter than 30 nucleotides. The reference genome in FASTA format was created by combining references *Homo sapiens* (GRCH 38 v89), *A. fumigatus* Af293 (s03-m05-r09) and human herpesvirus 5 strain TB30/E clone TB40-BAC4 (EF999921.1). Reference annotation was created by extracting and combining exon features from corresponding annotation files. The reference genome was indexed with exon information using HiSat2 version 2.1.0. Paired-end read alignment used HiSat2 on the created reference genome. Only concordantly aligned pairs of reads were used. Mapping statistics per organism were calculated using the "calc_triple_mapping_stats" function of GEO2RNaseq. SAMtools version 1.7 with the "flagstat" subcommand was used to deduce alignment quality. Gene abundance estimation was done with featureCounts (*R* package Rsubread version 1.28.0) in paired-end mode with default parameters. MultiQC version 1.5 was used to summarize the output of FastQC, Trimmomatic, HiSat, featureCounts and SAMtools (Data S1). In addition to the count matrix with gene abundance for all three species, species-specific gene count matrices were extracted

from the complete count matrix. For nonstatistical analyses, count matrices were normalized using median-by-ratio normalization (MRN) as described before (Anders and Huber, 2010). Correlation analysis, principal component analysis, and clustering were performed per species based on MRN gene-abundance data. Clustering between samples used the complete linkage (farthest neighbor) method. Raw files are accessible under the Gene Expression Omnibus accession number GSE134344, GSE135450 and GSE136217.

Differential gene expression analysis

Differential gene expression was analyzed by GEO2RNaseq per species. Pairwise tests were performed between control, single-infection, and co-infection groups with and without consideration of infection time. Four statistical tools (DESeq 1.30.0, DESeq2 1.18.1, limma voom 3.34.6 and edgeR 3.20.7) were used, and p values were corrected for multiple testing using the false-discovery rate method q = FDR(p) for each tool. In addition, mean MRN, transcripts per kilobase million (TPKM) and reads per kilobase million (RPKM) values were computed per test per group including corresponding $\log_2$ fold-changes. Gene expression differences were considered significant if they were reported significant by all four tools ($q < 0.01$ and $|\log_2 \text{MRN}| \geq 1$ for *H. sapiens*; $q < 0.05$ for *A. fumigatus* and CMV).

To compare RNA-seq and qRT-PCR derived relative differences, expression values were scaled by the maximum value per replicate. To keep statistical analysis comparable, significance was assessed based on pairwise t tests. Resulting p values were corrected for multiple testing using FDR. Tests were performed individually for RNA-seq and qRT-PCR per gene (Figure 5; Figure S5).

Interspecies and intraspecies gene expression analyses

Abundances of genes with nonzero coverage from all three species and all samples were MRN normalized. Spearman's correlations between gene abundances were calculated per treatment group (moDC, moDC + *A. fumigatus* [Afu], moDC + CMV, moDC + CMV + Afu) for infection time 0 h. Only significant correlations with $p < 0.01$ and absolute correlation $\geq 30\%$ were used for further analysis. *R* package iGraph version 1.2.4.1 was used to create, compare, analyze (node degree and betweenness) and plot significant correlations as networks. Node degree centrality describes the number of edges incident to a node. Node betweenness centrality describes the number of shortest paths through a node for all pairs of nodes. For cross-species analysis, correlations between genes of the same species were ignored. For additional immune system relevant gene correlation analysis, genes from *H. sapiens* were retained only if they were present in the curated database InnateDB (https://www.innatedb.com/). moDC gene set analysis with distinct expression patterns between, but low variance within different infection etiologies yielded 160 genes that were further filtered for immune system-relevant genes (Figure 4).